
Chromatic and luminance interactions in spatial contrast signals

JONATHAN D. VICTOR, KEITH P. PURPURA, AND MARY M. CONTE

Department of Neurology and Neuroscience, Cornell University Medical College, New York

(RECEIVED August 28, 1997; ACCEPTED December 3, 1997)

Abstract

We report VEP studies which delineate interactions between chromatic and luminance contrast signals. We examined responses to sinusoidal luminance gratings undergoing 4-Hz square-wave contrast reversal, upon which standing gratings with various admixtures of luminance and chromatic contrast were alternately superimposed and withdrawn. The presence of the standing grating induced a VEP component at the fundamental frequency of the contrast-reversal grating. This VEP component appeared without any appreciable lag, and did not vary in amplitude over the 4 s during which the standing grating was present. The observed fundamental response differed from the fundamental component that would be expected from the known interaction between the luminance component of the standing grating with the modulated grating (Bodis-Wollner et al., 1972; Bobak et al., 1988), in three ways: (1) The fundamental response was not nulled for standing gratings that were isoluminant or near-isoluminant. (2) The chromatic dependence of the fundamental response implied an S-cone input to the interaction. (3) No single mechanism (driven by a linear combination of cone signals) could account quantitatively for the size of this response, particularly when the standing grating strongly modulated two cones in phase.

Keywords: Chromatic contrast, Luminance contrast, Isoluminance, Evoked potentials

Introduction

The visual system adjusts its response characteristics not only to changes in ambient illumination (Shapley & Enroth-Cugell, 1984; Walraven et al., 1990), but also to changes in ambient contrast (Shapley & Victor, 1979). As recently reviewed (Victor et al., 1997), this dynamic adjustment serves the dual role of improving signalling efficiency and conditioning the incoming sensory data for central feature detection.

Adaptive changes to luminance are widely appreciated, and have been studied at many levels of the visual system (reviewed in Shapley & Enroth-Cugell, 1984; Walraven et al., 1990). Adaptive changes to luminance contrast, though more recently recognized, are widespread, across species (Shapley & Victor, 1978; Sclar et al., 1989; Benardete et al., 1992; Smirnakis et al., 1997; Victor et al., 1997) and processing stages (Shapley & Victor, 1981; Albrecht & Hamilton, 1982; Ohzawa et al., 1982, 1998; Albrecht et al., 1984; Sclar et al., 1989; Reid et al., 1992; Conte et al., 1997). However, of equal importance for human vision, natural visual scenes differ not only in luminance and contrast, but also in their chromatic aspects. Adaptive changes to shifts in chromatic background have attracted much interest, often in the context of “color

constancy” (Boynton, 1979; Blackwell & Buchsbaum, 1988; Brainard & Wandell, 1992; Wandell, 1995; Webster & Mollon, 1995). However, adaptive changes to chromatic contrast (without shifts in mean chromaticity) are largely unexplored.

One possibility is that the contrast gain controls at all stages of processing in the human visual system ignore purely chromatic contrast, and that the adjustments that they make in visual processing reflect only the luminance contrast in the visual scene. However, the apparent contrast of a central patch is reduced by isoluminant chromatically modulated surrounds (Singer et al., 1993; D’Zmura et al., 1995; Singer & D’Zmura, 1994, 1995). This phenomenon is most prominent when the surround is modulated in the same direction as the patch, but also occurs when the surrounding region is modulated in a near-isoluminant direction, and the patch is achromatic. Furthermore, an adaptive change (which affects processing of luminance and color) induced by chromatic contrast signals is, by definition, an interaction between chromatic and luminance mechanisms, and is therefore relevant to understanding interactions between chromatic and luminance signals that have been demonstrated psychophysically (Cole et al., 1990; Switkes et al., 1988).

In these studies, we examine the effects of chromatic contrast on the processing of luminance contrast signals in humans. Since our VEP approach makes use of temporal modulation to distinguish between luminance and chromatic stimulus components, we are able to examine the effects of spatially superimposed chromatic

Reprints requests to: Jonathan D. Victor, Department of Neurology and Neuroscience, Cornell University Medical College, 1300 York Avenue, New York, NY 10021, USA.

and luminance contrast. Additionally, since our stimulus and analysis paradigm is similar to that of a paradigm from a recent study (Victor et al., 1997) of the (luminance) contrast gain control, we are able to make a direct comparison of the dynamics of these two adaptive changes. As we will show, this comparison reveals facilitatory interactions that cannot be viewed simply as chromatic inputs to previously defined gain controls that are sensitive to luminance contrast.

Methods

Visual stimuli

The visual stimulus consisted of a luminance grating, upon which a standing chromatic grating was alternately superimposed and withdrawn (Fig. 1). The luminance grating (2.3 cycles/deg, contrast 0.125 $[(I_{\max} - I_{\min}) / (I_{\max} + I_{\min})]$) underwent square-wave contrast reversal at a temporal frequency of 4.22 Hz. The chromatic grating was a sinusoidal grating of the same spatial frequency and spatial phase, superimposed on the luminance grating for 16 periods of contrast reversal (3.79 s) and then removed for 16 periods, as indicated in Fig. 1. This constituted a single stimulus cycle (7.58 s). A single run consisted of eight continuous presentations of this stimulus cycle, preceded by a 5-s period of stimulus presentation during which no data were collected, for a total of 65.61 s. In essence, our stimulus consisted of a parametrically varied chromatic/luminance grating that appeared and disappeared for periods of 3.79 s, superimposed on a continuously present luminance grating modulated sinusoidally at 4.22 Hz. This approach may limit the observable interactions (since transient color mechanisms are ignored) and precludes separation of interaction of various formal orders by their frequency. However, it permits a direct examination of the timecourse of the overall interaction, as described below.

The R, G, and B components of the chromatic grating were varied parametrically from run to run, as described below. In all cases, the chromatic grating was counterphase, and modulated about the same white point as the luminance grating. Recordings

were organized into seven sessions, and the color coordinates used for each session are summarized in Table 1, and illustrated in Fig. 2. In two sessions, the chromatic grating was an R/G counterphase grating, with the R:G ratios chosen from a sequence which crossed the isoluminant plane (at high resolution in the "R/G, 2%" session; at lower resolution in the "R/G, 3%" session). In the third session (the "B/G" session), the chromatic grating was a B:G counterphase grating, with the B:G ratios chosen from a sequence which crossed the isoluminant plane. In the fourth session ("diagonals"), the R, G, and B guns were modulated equally, but at various depths and in all possible relative polarities. That is, the four color directions (+R+G+B; +R-G+B; +R+G-B; +R-G-B) were directed along the long diagonals of a cube in RGB space. For these sessions, the color coordinates used can be read directly from Table 1.

For the last three sessions, color directions were specified in a cardinal color space (Derrington et al., 1984). In the fifth and sixth sessions ("CIE isoluminant circle" and "personalized isoluminant circle"), color directions were chosen to lie in a circle within the isoluminant plane, as determined from CIE standard tables or from the subjects' isoluminant matches (Table 2). The color directions were equally separated by 22.5 deg, with a ninth direction at 101.25 deg (near the S-isolating direction) to ensure that the experiment included at least one direction in which R and G guns were modulated in phase. In the seventh session ("CIE cylinder"), color directions were chosen to point towards a circle parallel to the isoluminant plane. These color directions were the vector sum of a white light and one half of the isoluminant modulations used in the "CIE isoluminant circle" session. For these sessions, the color coordinates used are determined by summing the R,G,B triples for the cardinal color coordinates (specified in Table 3) after weighting by the directions listed in Table 1.

Note that all seven sessions included runs in which the superimposed grating was achromatic (R, G, and B components equal). Additionally, the B/G session included the S-cone-isolating stimuli from the CIE isoluminant circle session and the personalized isoluminant circle session. These duplications enabled us to verify consistency of responses across sessions.

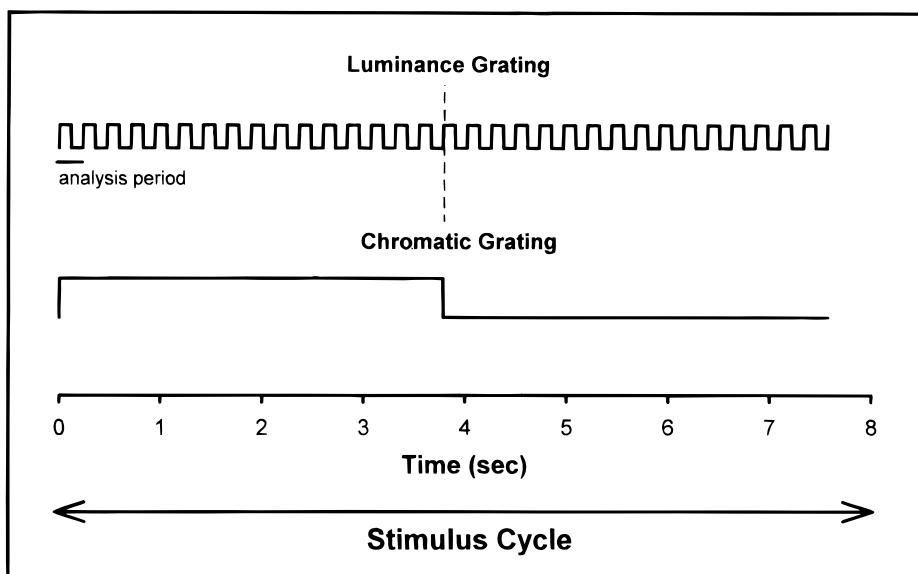


Fig. 1. The basic experimental design. The stimulus consisted of two superimposed components: a luminance grating, which underwent square-wave contrast reversal at a temporal frequency of 4.22 Hz, and a chromatic grating, which was superimposed on the luminance grating for 16 periods of contrast reversal (3.79 s) and then removed for 16 periods.

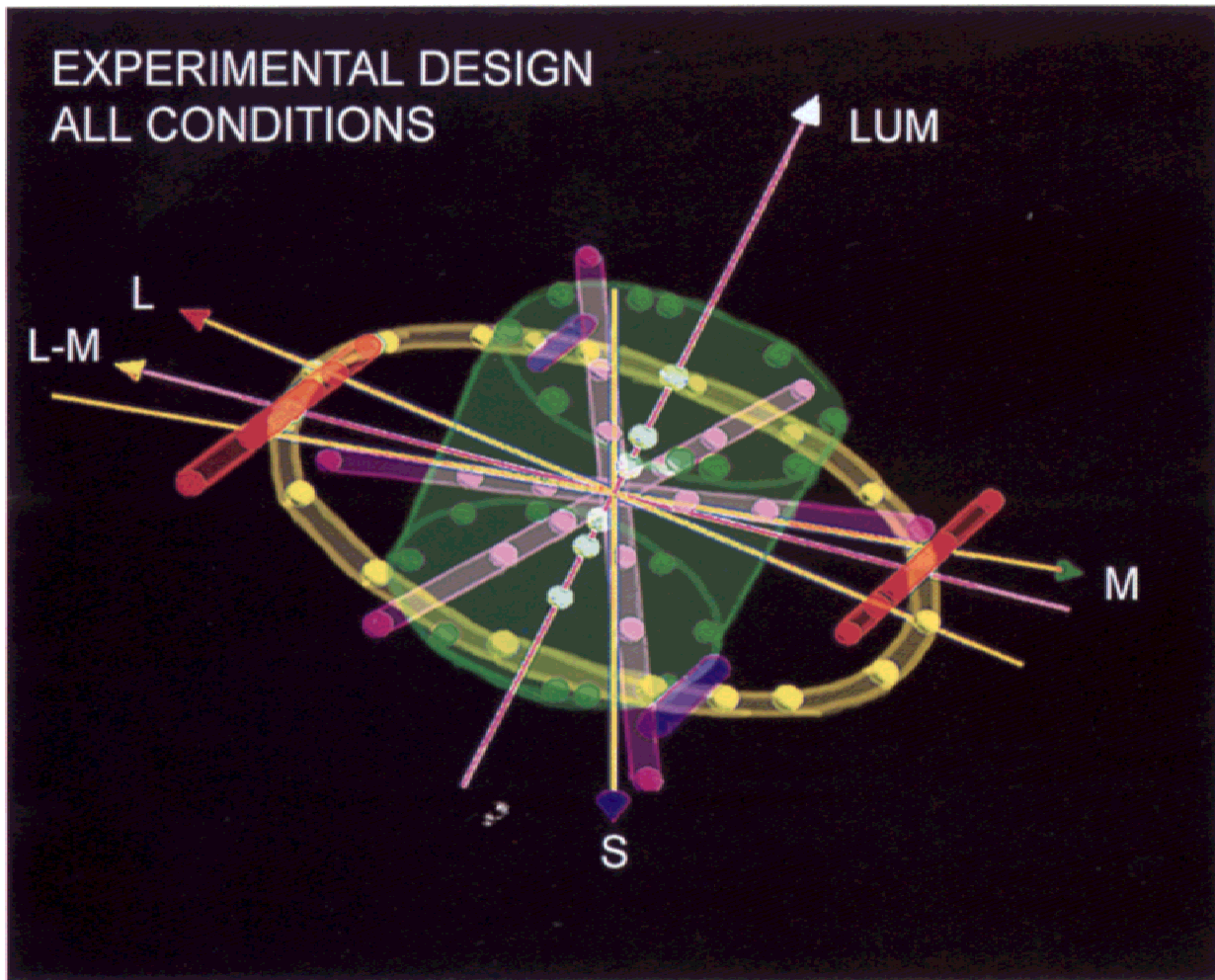


Fig. 2. The color coordinates used in these experiments (Table 1), displayed in a cardinal color space (Derrington et al., 1984) based on CIE fundamentals. Points corresponding to the R/G sessions are red; points corresponding to the B/G sessions are blue; points corresponding to the diagonals are purple; points corresponding to the isoluminant circle are yellow; points corresponding to the cylinder session are green; and points corresponding to the achromatic stimuli common to the sessions are white.

These visual stimuli were produced on a 256×256 pixel raster on a Conrac 7351. The display subtended 14 deg at a viewing distance of 114 cm and had a mean luminance of 53 cd/m^2 and a frame rate of 135 Hz. Control signals for the stimulator were produced by specialized electronics, modified from the design of Milkman et al. (1980) interfaced to a DEC computer. These electronics included a digital look-up table which corrected for the individual nonlinear intensity/voltage relationship of the R, G, and B guns, as determined empirically by a photocell. The spectral emission characteristics of the phosphors were measured by a Pritchard 703A spectrophotometer at the beginning of the series of experiments; luminance and CIE chromaticity values are provided in Table 4. Stability over the duration of the experiment was monitored by repeating flicker photometry prior to every experimental session.

It is recognized that certain CRT nonlinearities persist despite look-up table correction (Pelli & Zhang 1991; Naiman & Makous, 1992; see also Table 4). The superimposition of the luminance and chromatic gratings were realized by presenting these gratings on alternate frames, to minimize any artifactual nonlinear interactions

related to nonideal behavior of the CRT. Each frame had a duration of approximately 7.4 ms. During the epochs in which the chromatic grating was not present, the corresponding interleaved frames consisted of a uniform display of the mean luminance. Thus, actual contrasts were limited to 0.5, and all frames had an identical mean luminance. (Note that the contrasts specified in Table 1 and the figures correspond to single-frame contrasts, which should be multiplied by 0.5 to yield the effective contrast of the interleaved stimulus.) Additionally, we determined spectrophotometrically that with all gun signals at the maximum used in these experiments, additivity (in a noninterleaved display) was maintained to within 2%.

Color calibrations

The correspondence of R-, G-, and B-gun emissions and cone absorptions was established by spectrophotometric measurements of the CRT light output and digital convolution with cone fundamentals (Smith & Pokorny, 1975; Boynton, 1979 (p. 404); Schnapf et al., 1987). Cone-isolating directions determined in our lab in this fashion have been confirmed in anomaloscopically verified dichro-

Table 1. Color directions^a

Session		Coordinates for chromatic gratings			Coordinates for achromatic gratings		
R/G, 2%		R	G	B	R	G	B
		1.00	0.00	0.00	0.031	0.031	0.031
		1.00	-0.12	0.00	0.50	0.50	0.50
		1.00	-0.20	0.00			
		1.00	-0.25(*)	0.00			
		1.00	-0.27	0.00			
		1.00	-0.29	0.00			
		1.00	-0.31	0.00			
		1.00	-0.33	0.00			
		1.00	-0.35(**)	0.00			
	1.00	-0.40	0.00				
	1.00	-0.60	0.00				
R/G, 3%		R	G	B	R	G	B
		1.00	0.00	0.00	0.25	0.25	0.25
		1.00	-0.12	0.00	0.50	0.50	0.50
		1.00	-0.22	0.00			
		1.00	-0.25	0.00			
		1.00	-0.28	0.00			
		1.00	-0.31	0.00			
		1.00	-0.34	0.00			
		1.00	-0.37	0.00			
		1.00	-0.40	0.00			
	1.00	-0.60	0.00				
B/G		R	G	B	R	G	B
		0.00	0.00	1.00	0.125	0.125	0.125
		0.00	-0.04	1.00	0.25	0.25	0.25
		0.00	-0.08	1.00	0.50	0.50	0.50
		0.00	-0.10	1.00			
		0.00	-0.12	1.00			
Diagonals		R	G	B	R	G	B
		0.125	-0.125	0.125	0.125	0.125	0.125
		0.25	-0.25	0.25	0.25	0.25	0.25
		0.50	-0.50	0.50	0.50	0.50	0.50
		0.125	0.125	-0.125			
		0.25	0.25	-0.25			
		0.50	0.50	-0.50			
		0.125	-0.125	-0.125			
		0.25	-0.25	-0.25			
		0.50	-0.50	-0.50			
CIE Isoluminant circle	Polar angle	LM-CIE	S-CIE	White	R	G	B
	0.0	1.00	0.00	0.00	0.125	0.125	0.125
	22.5	0.9239	0.3827	0.00	0.25	0.25	0.25
	45.0	0.7071	0.7071	0.00	0.50	0.50	0.50
	67.5	0.3287	0.9239	0.00			
	90.0	0.00	1.00	0.00			
	101.3	-0.1951	0.9808	0.00			
	112.5	-0.3287	0.9239	0.00			
	135.0	-0.7071	0.7071	0.00			
	157.5	-0.9239	0.3827	0.00			
Personalized Isoluminant circle	Polar angle	LM-pers	S-pers	White	R	G	B
	0.0	1.00	0.00	0.00	0.125	0.125	0.125
	22.5	0.9239	0.3827	0.00	0.25	0.25	0.25
	45.0	0.7071	0.7071	0.00	0.50	0.50	0.50
	67.5	0.3287	0.9239	0.00			
	90.0	0.00	1.00	0.00			
	101.3	-0.1951	0.9808	0.00			
	112.5	-0.3287	0.9239	0.00			
	135.0	-0.7071	0.7071	0.00			
	157.5	-0.9239	0.3827	0.00			

(continued)

Table 1 *Continued*

Session		Coordinates for chromatic gratings			Coordinates for achromatic gratings		
CIE cylinder	Polar angle	LM-CIE	S-CIE	White	R	G	B
	0.0	0.50	0.00	0.50	0.125	0.125	0.125
	45.0	0.3535	0.3535	0.50	0.25	0.25	0.25
	90.0	0.00	0.50	0.50	0.50	0.50	0.50
	101.3	-0.0975	0.4904	0.50			
	135.0	-0.3535	0.3535	0.50			
	180.0	-0.50	0.00	0.50			
	225.0	-0.3535	-0.3535	0.50			
	270.0	0.00	-0.50	0.50			
	282.3	0.0975	-0.4904	0.50			
	315.0	0.3535	-0.3535	0.50			

^aThe color directions used for the superimposed gratings, and how they were organized into sessions. Each session included runs with superimposed chromatic gratings (left set of coordinates) and runs with superimposed achromatic gratings (right set of coordinates). Note that some stimuli are specified in R, G, and B coordinates (the gun directions of the CRT), and others by cardinal chromatic axes, as indicated by the column headers. CIE, LM-CIE, and S-CIE indicate modulation along the L-M and S-isolating directions in the Derrington et al. (1984) system, with the transformation from gun directions to cone-isolating directions determined by CIE values. LM-pers and S-pers indicate modulation along the corresponding DKL directions, but with the transformation from gun directions to cone-isolating directions determined by individual isoluminant matches. These transformations are provided in Table 3, and are derived from the flicker photometric data of Table 2 as described in the text. For the color directions defined by DKL coordinates, the polar angle indicates the angle between the LM-axis and the projection of the color direction into the isoluminant plane (0 deg = LM-isolating, 90 deg = S-isolating). In all cases, a contrast of 1.0 indicates the maximal available contrast from the CRT in the indicated color direction. Note that since the chromatic grating was presented in interleaved frames, the effective (time-averaged) depth of modulation is half of the values presented in the tables. (*) indicates a condition omitted for subject JV; (**) indicates a condition included only for subject JV.

mats (Purpura & Victor, 1990) and by the fading of an S-isolating contour in the central fovea. Cardinal color axes (Derrington et al., 1984) and cone absorptions determined in this fashion will be denoted "CIE."

Additionally, for each observer, we used the following procedure to determine a set of "personalized" color axes and cone absorptions (Table 2), based on the assumption that individual differences were due to differences in preretinal absorptions (see Discussion). We used flicker photometry at 16 Hz to determine the amount of counterphase G modulation required to match sinusoidal modulation of the R and B guns at a contrast of 0.5. Subjects were instructed to minimize the apparent flicker near the fixation point. Measurements were made for full-field gratings identical to those used in the experiments (with the subjects instructed to minimize the apparent flicker near the fixation point), but modulated at 16 Hz, as well as 2-deg spots. We then multiplied the standard

L, M, and S absorption spectra by absorption factors for the lens and macula (Wyszecki & Stiles, 1967, p. 719). The assumed "thickness" of the lens and macula were allowed to vary separately (by applying overall multipliers to the tabulated optical densities) until simultaneous exact matches to the empirical R:G and B:G ratios were obtained. These modified, or "personalized," cone fundamentals enabled us to construct a "personalized" cardinal color space in which the isoluminant plane was matched to the observer's isoluminance judgements, and in which cone-isolating directions were approximately corrected for the observer's preretinal absorptions. For both the CIE and personalized coordinate systems, the vector difference between the L-isolating and M-isolating direction was taken as a vector along the L-M direction. This vector and the S-isolating vector obtained directly from the CIE fundamentals were then rescaled so that the maximum of the three gun modulations was equal to 1.0. The results of these calculations are summarized in Table 3.

Table 2. *Flicker photometry*^a

Subject	2 cycles/deg grating		2-deg disk	
	R/G	B/G	R/G	B/G
CIE			0.269	0.123
CM	0.310	0.126	0.311	0.137
JV	0.344	0.088	0.334	0.103
MC	0.307	0.095	0.375	0.084
RR	0.385	0.106	0.365	0.144

^aFlicker photometric data. The ratio of counterphase modulation of the G gun required to minimize heterochromatic flicker. Measurements were made at a modulation depth of 0.5 for the R and B guns of a Conrac 7351 monitor. The entries labelled "CIE" are calculated as described in Methods.

Subjects and VEP recording

Studies were conducted in four normal subjects (2 male, 2 female) who ranged in age from 20 to 40 years, and had visual acuities (with correction if necessary) of 20/20 or better. Scalp signals were obtained from standard gold cup electrodes, applied to the scalp with Nihon-Kohden electrolyte paste at C_z (+) and O_z (-). Electroencephalographic activity was amplified 10,000-fold, filtered (0.03 to 100 Hz) and digitized at the frame rate. Digitized data were segmented into epochs consisting of one cycle of contrast reversal (64 bins, or 0.237 s, at 4.22 Hz) for Fourier analysis. Confidence limits of the Fourier coefficients were determined off-line by the T_{circ}^2 statistic (Victor & Mast, 1991). Parameter optimization for the models was performed in Microsoft Excel versions 4 and 5.

Table 3. Color space transformations^a

	Subject	R	G	B
L isolating	CIE	0.2541	-0.0324	-0.0003
	CM	0.2668	-0.0379	0.0007
	JV	0.2738	-0.0426	0.0035
	MC	0.2641	-0.0375	0.0015
	RR	0.2839	-0.0475	0.0036
M isolating	CIE	-0.4037	0.1461	-0.0125
	CM	-0.4302	0.1811	-0.0212
	JV	-0.4531	0.2114	-0.0397
	MC	-0.4296	0.1779	-0.0255
	RR	-0.4725	0.2449	-0.0426
S isolating	CIE	0.7434	-0.7339	4.3279
	CM	0.9836	-1.0947	6.2505
	JV	1.2144	-1.927	17.1481
	MC	0.9897	-1.3054	10.5438
	RR	1.3422	-1.9882	13.7973
L-M (max)	CIE	1.0000	-0.2714	0.0185
	CM	1.0000	-0.3142	0.0314
	JV	1.0000	-0.3494	0.0594
	MC	1.0000	-0.3105	0.0389
	RR	1.0000	-0.3866	0.0611
S isolating (max)	CIE	0.1718	-0.1696	1.0000
	CM	0.1574	-0.1751	1.0000
	JV	0.0708	-0.1124	1.0000
	MC	0.0939	-0.1238	1.0000
	RR	0.0973	-0.1441	1.0000
White	All	1.0000	1.0000	1.0000

^aColor space transformations. The L, M, and S cone-isolating directions were determined from standard Smith-Pokorny fundamentals (labelled "CIE"), or from fundamentals as modified to match the flicker photometric data determined for each subject (Table 2). The "L-M (maximum)" direction was determined by subtracting the corresponding cone-isolating directions, and rescaling the (R, G, B) triplet to achieve a maximum modulation depth ($R = 1.0$). The "S (maximum)" direction was determined by rescaling the (R, G, B) triplet for the S-isolating direction to achieve a maximum modulation depth ($B = 1.0$).

Results

Responses to luminance contrast on a chromatic background

Fig. 3 shows a detailed analysis of the VEP waveforms elicited by a contrast reversal luminance grating with and without a superimposed chromatic grating. The waveforms represent averages across a total of 64 passes through each epoch (1 cycle of contrast reversal of the luminance grating). These 64 passes were accumulated in continuous runs of eight passes each, and there were eight replicate runs of each experimental condition per session. Epochs 1 (0–0.24 s) and 17 (3.8–4.03 s) immediately followed the introduction (epoch 1) and removal (epoch 17) of the standing chromatic grating. Responses from these epochs, as well as the immediately following epochs (epoch 2: 0.24–0.47 s, and epoch 18: 4.03–4.27 s), are separately averaged. Responses from the later epochs are pooled (epochs 3–4: 0.47–0.95 s; epochs 5–16: 0.95–3.8 s; epochs 19 and 20: 4.27–4.74 s; epochs 21–32: 4.74–7.58 s) to improve signal to noise.

In the second half of the figure (epochs 17–32: 3.8–7.58 s), there is no standing chromatic grating. With the exception of epoch

Table 4. CRT characteristics^a

	R	G	B	W
Luminance (cd/m^2)	10.3	38.3	4.5	52.7
x	0.624	0.291	0.152	0.303
y	0.348	0.613	0.077	0.353

^aLuminance and chromaticity (CIE 1931) characteristics of the CRT used in this study, as determined by measurements with a Pritchard 703A spectrophotometer for each gun separately at its mean intensity, and for the three guns together (labelled W). The superposition of the three guns at their mean constituted the white point for these experiments. Note that there is a slight deviation from linearity: the total luminance of the three guns individually is 53.0 cd/m^2 , but the measured luminance of the white point is 52.7 cd/m^2 .

17 (which begins with the removal of the standing chromatic grating at 3.8 s), the stimulus is simply a contrast-reversing luminance grating, whose contrast is fixed at 0.125. Thus, one anticipates that the response in these epochs will be identical at the two phases of contrast reversal, i.e. the standard even-harmonic response to contrast reversal (Spekreijse et al., 1973; Regan, 1989). As is seen in Fig. 3, this is approximately the case. A multitude of mechanisms may contribute to these harmonics, including nonlinearities in the contrast-response function and response to local flicker. As seen in Fig. 3, even harmonic components (primarily F2) are present both with and without the superimposed chromatic grating.

In epochs 1–16 (0–3.8 s), the contrast-reversing luminance grating is superimposed on a standing grating, which contains both luminance and chromatic components. This compound stimulus may be decomposed into a stimulus confined to the isoluminant plane, and a pure luminance stimulus. We initially assume that these components do not interact. Only the standing chromatic grating contributes to the component within the isoluminant plane. Since it is not modulated in time (except at the onset of epoch 1), it cannot lead to modulated components of the VEP. Now consider the luminance component of the stimulus. The standing grating, which is in color direction $(R, G, B) = (1.00, 0.00, 0.00)$, has an effective luminance contrast of approximately 0.15. When a contrast-reversing luminance grating at a contrast of 0.125 is superimposed on this pattern, the effective contrast is modulated between approximately 0.275 and 0.025. The largest contrast, approximately 0.275 ($= 0.15 + 0.125$), is achieved in the first half of each epoch, when the luminance components of the two gratings reinforce. The smallest contrast, approximately 0.025 ($= 0.15 - 0.125$), is achieved in the second half of each epoch, when the luminance components of the two gratings nearly cancel. Thus, one expects (Bodis-Wollner et al., 1972; Spekreijse et al., 1973) that the luminance component of the stimulus will generate a VEP with a strong first-harmonic (F1) component, corresponding to this substantial contrast modulation. Indeed, a first-harmonic component is apparent in epochs 2–16 of the response (see odd harmonics of Fig. 3), as well as the even harmonic components described above.

Epochs 1 (0–0.24 s) and 17 (3.8–4.03 s) are transitional, in that they contain chromatic modulation (introduction or withdrawal of the standing grating). This modulated component generates a contribution to the VEP which likely superimposes on (and perhaps interacts with) the VEP elicited by the modulated luminance grating. As seen in Fig. 3, the responses measured in these epochs contain large odd harmonics, presumably because the chromatic response, whose latency is on the order of 100 ms, occurs in the

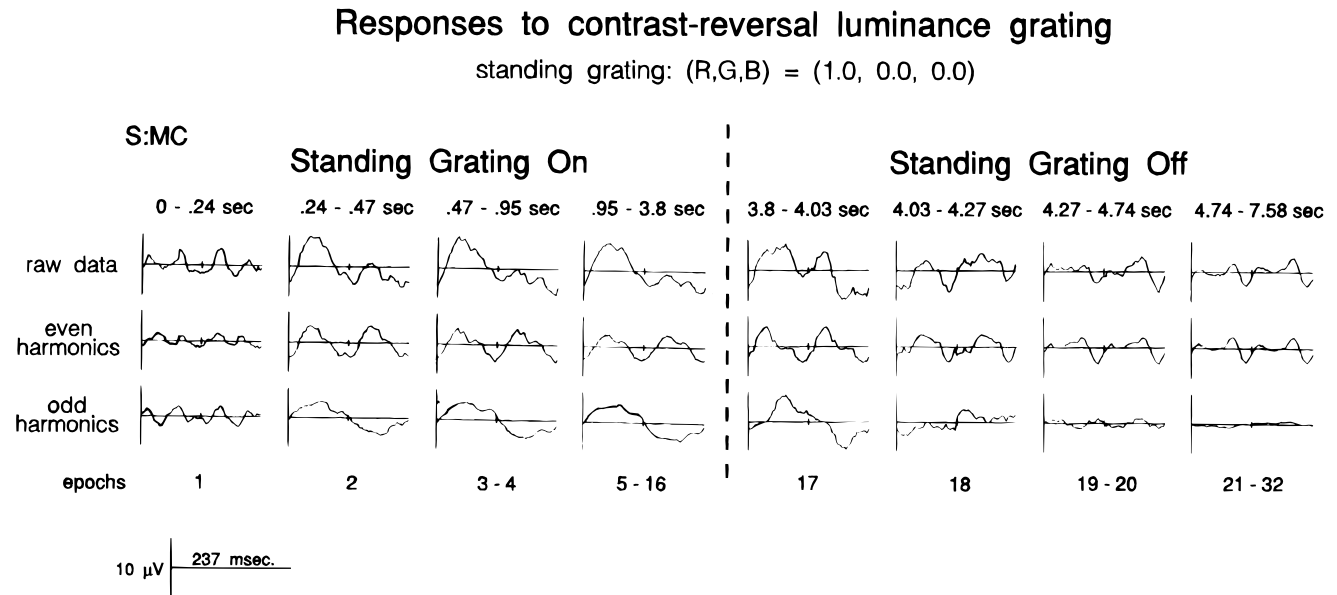


Fig. 3. Responses to contrast-reversal gratings with (left) and without (right) a superimposed chromatic grating. The chromatic grating had color coordinates (R, G, B) of (1.00, 0.00, 0.00). The traces labelled “even harmonics” are calculated by averaging the responses in the first and second half of each epoch; the traces labelled “odd harmonics” are calculated from one half of the difference between the responses in the first and second half of each epoch. Subject: MC.

second half of each epoch. We do not attempt to dissect the responses from these transitional epochs into their components.

The above observations are made more quantitative in Fig. 4. Panel A shows the first and second Fourier components from each of the 32 epochs (7.58 s) of the stimulus cycle. In the first half of the stimulus cycle, during the time in which the standing chromatic grating is superimposed on the modulated luminance grating, there is a substantial fundamental response, with a consistent phase. When the superimposed grating is withdrawn, the first-harmonic amplitude drops essentially to zero, and its phase becomes random. For this dataset, the second harmonic has a larger amplitude in the first half of the epoch than in the second half. However, its amplitude does not drop to zero when the superimposed grating is withdrawn, and its phase remains consistent. Panel B shows comparable data collected under the condition that the superimposed grating is near isoluminance [(R, G, B) = (1.00, -0.25, 0.00)]. The amplitude behavior of the first harmonic does not show an obvious response in either half of the stimulus cycle, but the consistent phases in the first half of the cycle indicates that a response is indeed present. The second harmonic behaves in a manner similar to Panel A: responses are present, with consistent phases, in both halves of the stimulus cycle, and somewhat larger when the standing grating is present. Panel C shows data collected for a condition in which the counterphase G modulation dominates the luminance signal [(R, G, B) = (1.00, -0.40, 0.00)]. The response pattern is largely similar to Panel A, except that the phase of the fundamental in the first half of the stimulus cycle has shifted by half a cycle (approximately π radians) relative to the phase in Panel A. Note also that this dataset shows a 1-epoch transient in the second harmonic at the beginning of the stimulus cycle. As mentioned above, this represents a transient response to the onset of the chromatic grating, rather than a steady-state alteration of the contrast-reversal response to the luminance grating.

In a few datasets (e.g. Panel C), the fundamental response appeared to have an initial peak, prior to settling to a steady-state

value. However, this was not a constant finding, either within subjects (e.g. Panel A), or across subjects. When present, the size of these peaks was rarely significant by the T_{circ}^2 statistic (Victor & Mast, 1991). Thus, unlike the dynamic adjustment of the contrast-reversal VEP to increases and decreases in luminance contrast (Victor et al., 1997), the fundamental response induced by the presence of the standing chromatic grating was generally constant for the duration of its presence.

For further analysis of how this response depended on the chromatic composition of the superimposed grating, we examined the vector average of the fundamental response during the last 12 epochs of the first half of the stimulus cycle (0.95–3.8 s following the appearance of the chromatic grating). The first 0.95 s were omitted from the average to ensure that any transient response to the onset of the chromatic grating was excluded, as well as any possible transient component of the interaction of the standing and modulated gratings.

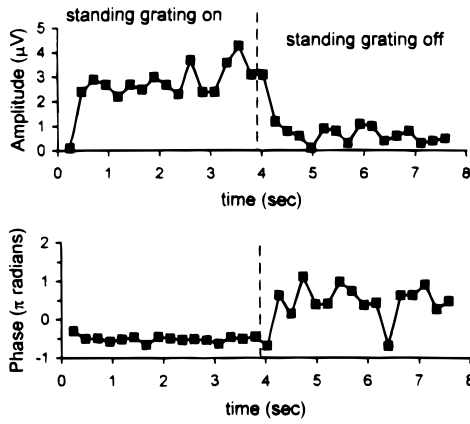
The hypothesis that luminance and chromatic components of the stimulus can be considered independently makes a straightforward prediction about the response to a modulated luminance grating superimposed on any standing grating. The prediction is that a fundamental response will be present when the standing grating has a luminance component, and that it should disappear when the standing grating is isoluminant. For example, as described above, a standing grating whose spatial contrast is produced by modulation of the red gun alone (Figs. 3 and 4A) has a luminance component. In the first half of the stimulus cycle (i.e. when this grating is superimposed on a contrast-reversing grating), the luminance contrast of the combined stimulus is modulated at the fundamental frequency, because of the alternate reinforcement and partial cancellation of the luminance components of the two stimulus components. However, if the standing chromatic grating were isoluminant, then there would be no modulation of luminance contrast at the fundamental frequency, even with superimposition of the two stimulus components.

Responses to contrast-reversal luminance grating

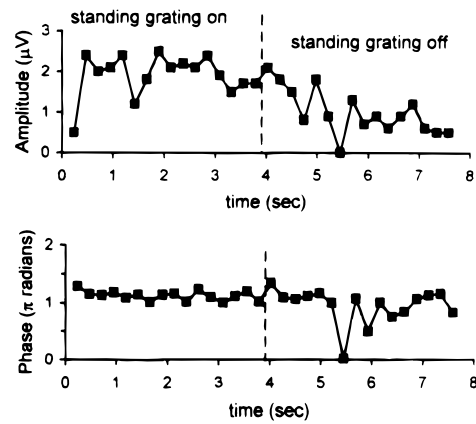
S:MC

standing grating: (R,G,B) = (1.0, 0.0, 0.0)

F1



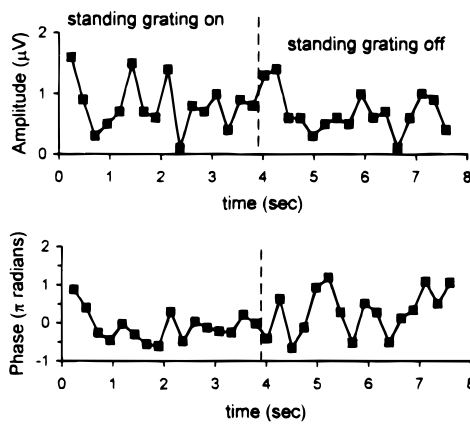
F2



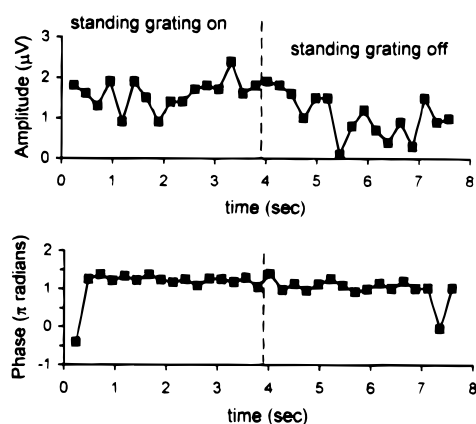
A.

standing grating: (R,G,B) = (1.0, -0.25, 0.0)

F1



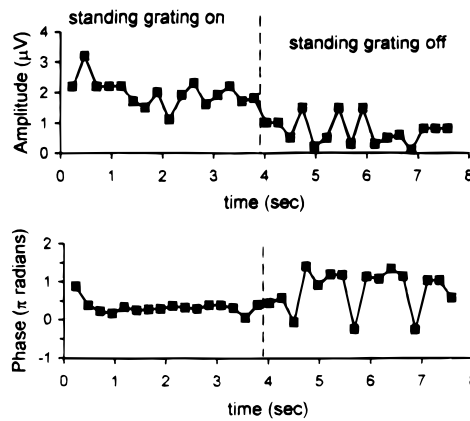
F2



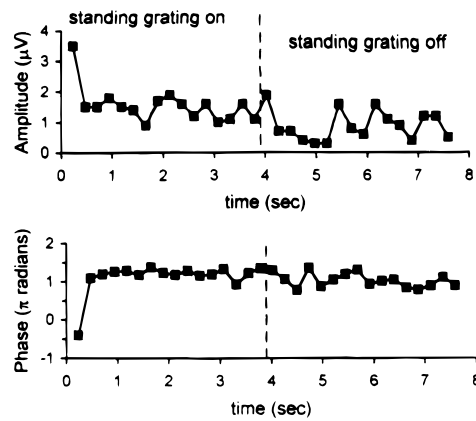
B.

standing grating: (R,G,B) = (1.0, -0.4, 0.0)

F1



F2



C.

FIGURE 4.

To test this idea, we plotted fundamental responses measured in the first half of each stimulus cycle as vectors (Fig. 5), parametric in the chromatic composition of the superimposed standing grating. One end of each trajectory corresponds to a superimposed grating that was produced by a single gun (the R gun in the left panels of Fig. 5, and the B gun in the right panels of Fig. 5). Along each trajectory, the amount of counterphase G modulation increased from 0 to an amount which dominated the luminance of the stimulus. If the fundamental response depended on the luminance component of the standing grating, the trajectory should pass through the origin at the isoluminant point. For the subject of Panel A, the radius of the 95%-confidence circle for the Fourier components, as determined by the T_{circ}^2 statistic, is $0.41 \mu\text{V}$. These confidence circles (not illustrated) do not include the origin for any of the R:G ratios (Fig. 5A, left) or B:G ratios (Fig. 5A, right). Furthermore, it is clear that the ratios have been sampled sufficiently closely so that the resulting trajectories deviate in a systematic way from the origin, rather than merely skipping over it. For the subject of Panel B, the radius of the 95%-confidence circle is $0.37 \mu\text{V}$. For this subject, the confidence circles include the origin for the smallest responses to both the R/G (Fig. 5B, left) and B/G gratings (Fig. 5B, right). Nevertheless, it is clear that the trajectory of points deviates in a systematic way from the origin. For the R/G gratings (Fig. 5B, left), all responses have a positive real part of approximately 0.2. For the B/G gratings (Fig. 5B, right), all responses have a positive real part and a negative imaginary part. In sum, while the hypothesis that the fundamental response depended solely on the luminance component of the standing grating predicts that the response trajectories should pass through the origin, in all cases, the observed responses deviate from the origin in a systematic fashion.

Fig. 5 also indicates the location of the subjective isoluminance point along each sweep. In all cases, the subjective isoluminance point differs from the closest approach of the trajectory to the origin (i.e. the gun ratio which yields the smallest response). For the R/G gratings (left side of Fig. 5), the gun ratio at isoluminance had a larger proportion of counterphase G than the gun ratio nearest the null. For the B/G gratings (right side of Fig. 5), the gun ratio at isoluminance had a smaller proportion of counterphase G than the gun ratio nearest the null.

To examine how the amplitude and phase of the induced fundamental behave as the chromatic composition of the superimposed grating varies throughout color space, we used a three-dimensional representation (Fig. 6). In this representation, the independent variable (the chromatic composition of the superimposed grating) is represented in DKL (Derrington et al., 1984) color space, with the isoluminant plane approximately horizontal. Each fundamental response is plotted within this space by a sphere, whose radius is proportional to the amplitude of the response, and whose color is determined by the phase of the response. Each experimental run generates two points in this space, since inversion of the color coordinates of the superimposed grating is equivalent to a half-cycle *spatial* phase shift of the modulated grating, which is in turn equivalent to a half-cycle *temporal* phase shift.

Examined in this manner, the data from all four subjects showed several features in common, as typified by the data from two subjects presented in Fig. 6. In general, responses far from the isoluminant plane are larger than responses which are near the isoluminant plane, but the distance from the isoluminant plane is not the sole determinant of response amplitude. Responses on each side of the isoluminant plane generally have similar phases (as indicated by their similar colors: blue and purple above the isoluminant plane; yellow below the isoluminant plane), but there are some responses that have intermediate phases, especially for the subject whose data are shown in Panel A.

Modelling the responses

The hypothesis of independence of luminance and chromatic signals predicts that the fundamental response is nulled at isoluminance. This is at variance with the observations of Fig. 5, which indicate that a fundamental response is present for a range of color directions which straddle the isoluminant plane. However, it may be possible to account for the bulk of the observations *via* a single mechanism which is sensitive to both the standing and modulated gratings, provided that chromatic sensitivities of this mechanism deviate from that of a pure luminance detector. If this mechanism's sensitivities are close to that of a luminance detector, it is unlikely that this is the entire explanation for the discrepancy. Any such hypothetical detector must have a null plane, and the color directions explored in the R/G and B/G sweep sessions would necessarily have straddled it. Thus, for a single mechanism (whose sensitivities deviate substantially from that of a luminance detector) to account for our results, its null plane must be far from any of the chromatic directions we have explored in the sweep sessions.

On the other hand, the overall features of Fig. 6 suggest that the single luminance-like mechanism idea may be approximately correct—distance from the isoluminant plane appears to correlate strongly with response amplitude, and response phase appears to be largely determined by whether the data point is above or below the isoluminant plane. A final alternative is that the hypothesis of a single mechanism sensitive to both stimulus components is wrong in a qualitative way, and that there are specific interactions between luminance and chromatic signals.

We now introduce a simple model, to analyze how well the observed responses can be accounted for by a single detector, either strictly sensitive to luminance or with a more general chromatic sensitivity. We assume that a standing grating, whose color direction is specified by gun modulations, m_R , m_G , and m_B , is detected by a mechanism whose relative sensitivities to R, G, and B modulation are determined by s_R , s_G , and s_B . That is, the response of this hypothetical mechanism to the standing modulated grating is assumed proportional to

$$D(m_R, m_G, m_B) = m_R s_R + m_G s_G + m_B s_B \quad (1)$$

(We normalize these relative sensitivities by the constraint $s_R^2 + s_G^2 + s_B^2 = 1$). The interaction between the standing grating

Fig. 4. Fourier analysis of responses to contrast-reversal gratings with and without a superimposed chromatic grating. Each point represents the Fourier components derived from one epoch (0.24 s) of the stimulus cycle. The chromatic grating had color coordinates (R, G, B) of (1.00, 0.00, 0.00) (Panel A), (1.00, -0.25, 0.00) (Panel B), and (1.00, -0.40, 0.00) (Panel C). Data of Panel A are taken from Fig. 3. Subject: MC.

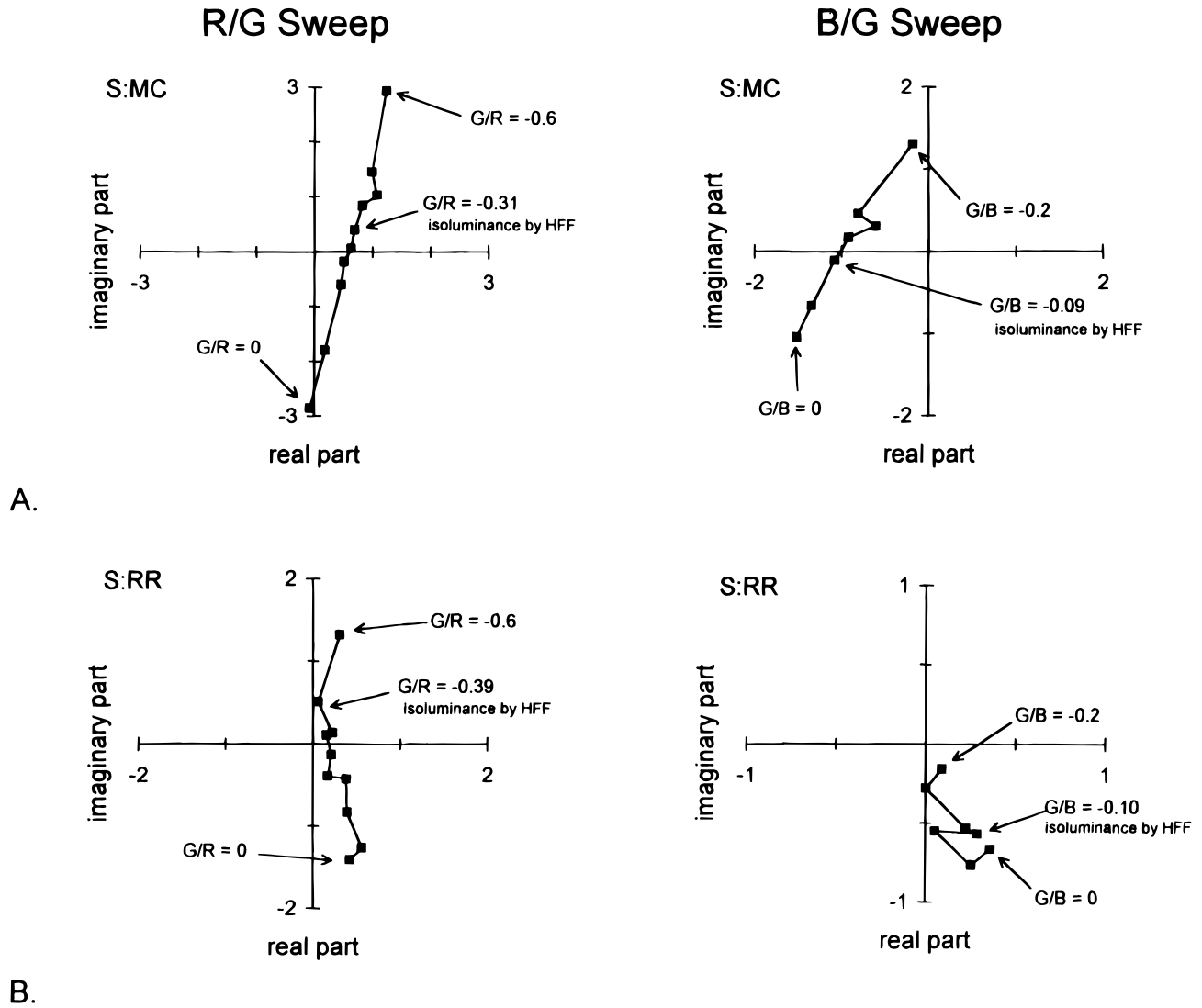


Fig. 5. Steady-state responses (first harmonics) elicited by contrast-reversal gratings superimposed on a series of chromatic gratings (R/G and B/G sessions). The locus of the vector which represents the amplitude and phase of the response does not pass through the origin (the point of a null response), and moves along a trajectory which indicates that the failure to pass through the origin is not a consequence of inadequate sampling of color space. The radius of the 95%-confidence circle about each response is $0.41 \mu\text{V}$ (Panel A) and $0.37 \mu\text{V}$ (Panel B). Panel A: subject MC. Panel B: subject RR.

and the modulated luminance grating is presumed to be determined solely by $D(m_R, m_G, m_B)$, since the luminance grating is constant in all experiments. We next postulate functional forms for the dependence of the amplitude and phase of the fundamental VEP component on $D(m_R, m_G, m_B)$. For amplitude, we use a form which encompasses a reasonably wide range of monotonic, saturating behaviors:

$$A(m_R, m_G, m_B) = \alpha^\sigma + \frac{|D(m_R, m_G, m_B)|^\sigma}{\beta^\sigma + |D(m_R, m_G, m_B)|^\sigma} \quad (2)$$

For phase, we assume a constant phase ϕ_0 at low contrast, and a gradually increasing (advancing) phase at high contrast, as might be expected from the action of the contrast gain control (Shapley & Victor, 1979). For simplicity, we assume that the amount of

phase advance is proportional to the contrast signal $D(m_R, m_G, m_B)$, and we denote the proportionality constant by ϵ :

$$\phi(m_R, m_G, m_B) = \phi_0 + \epsilon D(m_R, m_G, m_B) \quad (3)$$

We emphasize that our goal is not to suggest the mechanisms underlying the dependence of amplitude and phase on the postulated signal $D(m_R, m_G, m_B)$, but merely to enable a determination of the chromatic sensitivities (eqn. 1) of a single mechanism that might account for our findings.

The parameters $(s_R, s_G, s_B; \alpha, \beta, \sigma; \phi_0, \epsilon)$ provide an explicit prediction of the size of the fundamental response, under the hypothesis that it is generated by a mechanism with sensitivities (s_R, s_G, s_B) , and that the response *versus* signal behavior is specified by eqns. (2) and (3). To fit this model to the observed fun-

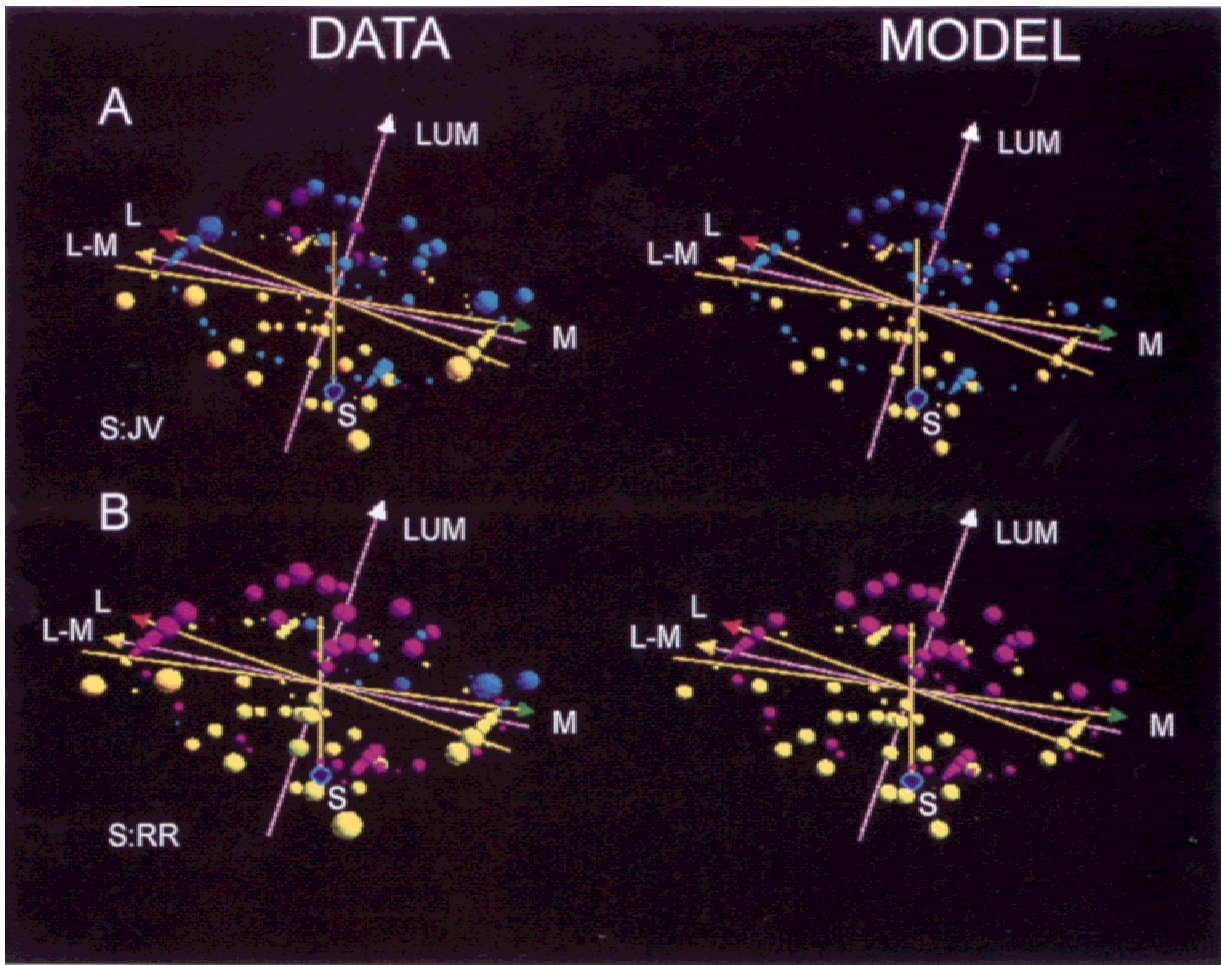


Fig. 6. Steady-state responses (first harmonics) elicited by contrast-reversal gratings superimposed on a series of chromatic gratings (all sessions), and a comparison with model predictions. The size of each sphere represents response amplitude, and its color represents response phase (red: in phase with the stimulus; yellow: quarter-cycle phase lead; green: out of phase; blue: quarter-cycle phase lag). The position of each sphere represents the chromatic and luminance content of the superimposed standing grating, and is plotted in a DKL coordinate system determined from CIE data. In each panel, the left side represents the observed responses and the right side represents the model fit. The model is defined by eqns. (1), (2), and (3), and model parameters are listed in Table 5. Panel A: subject JV. Panel B: subject RR.

damental responses, we sought parameter values which minimized the mean-squared error between the model predictions and the observed responses. Mean-squared error was averaged in an equally weighted fashion over all color directions, and was calculated from the vector difference between the observed response and the vector whose amplitude is given by eqn. (2), and whose phase is given by eqn. (3). Since the model has eight parameters and one constraint ($s_R^2 + s_G^2 + s_B^2 = 1$), we adopted the following strategy to avoid finding local minima. First, the sensitivities (s_R, s_G, s_B) were assumed to be that of a pure luminance mechanism, σ (the Michaelis-Menten exponent) was fixed at 1, and ϵ (the phase shift with contrast) was fixed at 0, and values of the main response parameters α, β , and ϕ_0 were determined by the Microsoft Excel (version 4 or 5) optimization routine. These values were found to be independent of the initial guesses supplied. Then, with β, σ, ϕ_0 , and ϵ held fixed at these values, the chromatic sensitivities (s_R, s_G, s_B) and overall amplitude parameter α were refined by the optimization routine (again, three parameters). Then, the chromatic sensitivities and phase parameters were held fixed, and the amplitude

parameters α, β , and σ were refined. Next, sensitivities and amplitude parameters (α, β, σ) were held fixed, and the phase parameters (ϕ_0, ϵ) were refined. After several cycles of refining the chromatic parameters, then the amplitude parameters, then the phase parameters, there was little shift in any of the parameters, as was confirmed by a joint optimization of all of the parameters of the model ($s_R, s_G, s_B; \alpha, \beta, \sigma; \phi_0, \epsilon$). Finally, the entire procedure was repeated with alternate initial guesses for the chromatic sensitivities, such as $(s_R, s_G, s_B) = (0, 1, 0)$. For each subject, all starting positions converged to a unique eight-parameter model, whose parameters are presented in Table 5.

We first consider the derived chromatic sensitivities. Relative sensitivities to R, G, and B guns (first three lines of Table 5) are qualitatively similar to the sensitivities needed to account for flicker photometry (Table 2). That is, R/G sensitivities of the derived mechanism range from 0.27:1 to 0.35:1 (compared with flicker photometric sensitivities of 0.31:1 to 0.38:1), and B/G sensitivities of the derived mechanism range from 0.13:1 to 0.18:1 (compared with flicker photometric sensitivities of 0.09:1 to 0.13:1).

Table 5. Model parameters^a

	Subject				Mean
	CM	JV	MC	RR	
Chromatic parameters					
s_R	0.327	0.321	0.256	0.325	0.307
s_G	0.936	0.935	0.958	0.930	0.940
s_B	0.131	0.150	0.129	0.171	0.145
Amplitude parameters					
α	1.96	2.27	2.27	1.09	1.90
β	0.089	0.078	0.081	0.083	0.083
σ	1.96	1.98	2.32	1.53	1.35
Phase parameters					
ϕ_0	1.36	1.27	1.26	1.52	1.35
ϵ	0.26	0.29	0.54	0.20	0.32
Normalized cone contributions (Q_L, Q_M, Q_S) to model mechanism sensitivities (s_R, s_G, s_B)					
CIE coordinates					
L	0.999	0.997	0.870	0.998	0.966
M	0.032	0.056	0.494	0.025	0.152
S	0.025	0.043	0.013	0.062	0.036
Personalized coordinates					
L	0.966	0.900	0.732	0.828	0.857
M	0.257	0.427	0.680	0.553	0.479
S	0.020	0.088	0.047	0.091	0.062
Normalized cone contributions ($Q_L, Q_M, 0$) to luminance sensitivities					
CIE coordinates					
L					0.876
M					0.482
Personalized coordinates					
L	0.883	0.896	0.889	0.909	0.894
M	0.470	0.445	0.459	0.417	0.448

^aFitted parameters for a model of the fundamental response as the result of a single mechanism which is sensitive to the chromatic background and the luminance grating. $s_R, s_G,$ and s_B represent the sensitivities of this putative mechanism to unit modulation of the three guns [eqn. (1)]. Amplitude is modelled by three parameters [eqn. (2)]: α (in microvolts) is the maximal VEP amplitude, β (in contrast units) is the semisaturation value, and σ is the power law for the contrast-response function at low amplitudes. Phase is modelled by two parameters [eqn. (3)]: ϕ_0 , the phase at low contrasts (in π radians) and ϵ , the rate of phase advance per unit response (in units of π radians per unit contrast). The lower portion of the table shows normalized cone contributions (Q_L, Q_M, Q_S) that reconstruct the observed sensitivities (s_R, s_G, s_B) of the model mechanism, as well as the normalized cone contributions that reconstruct an ideal luminance mechanism. For CIE coordinates, the normalized cone contributions for an ideal luminance mechanism are necessarily subject independent, and are listed only in the column labelled "mean." All coordinate triplets [(s_R, s_G, s_B) and (Q_L, Q_M, Q_S)] are normalized to have a vector length of 1.

To determine whether these relatively small deviations indicate a consistent discrepancy, we reexpressed the derived chromatic sensitivities (s_R, s_G, s_B) in terms of linear combinations of cone sensitivities. This is given by a triplet (q_L, q_M, q_S), which is linearly related to (s_R, s_G, s_B) by

$$q_c = \sum T_{cp} s_p \quad (4)$$

where T_{cp} is the modulation of gun p ($p = R, G,$ or B) required to isolate cone c ($c = L, M,$ or S), as given in Table 3. Were it the case

Table 6. Mean-squared modelling errors^a

	Subject			
	CM	JV	MC	RR
F1				
R/G, 2%	1.276*	0.806*	1.009*	0.148
R/G, 3%	0.456	0.821*	0.449*	0.125
B/G	0.724*	0.131	0.510*	0.074
Diagonals	1.640*	0.756*	0.583*	0.211
CIE isoluminant circle	0.329	0.354	0.338	0.083
Personalized isoluminant circle	0.298	0.250	0.283	0.063
Cylinder	0.334	0.250	0.204	0.042
Overall MSE	0.722	0.481	0.482	0.107
95% confidence limit	0.486	0.381	0.405	0.365
F2				
R/G, 2%	0.421*	0.277*	1.074*	0.172
R/G, 3%	0.254	0.172	0.681*	0.102
B/G	0.409*	0.112	0.721*	0.054
Diagonals	0.722*	0.080	0.277	0.139
CIE isoluminant circle	0.551*	0.114	1.074*	0.152
Personalized isoluminant circle	0.512*	0.165	1.309*	0.147
Cylinder	0.325	0.061	0.069	0.059
Overall MSE	0.456	0.140	0.744	0.118
95% confidence limit	0.375	0.197	0.279	0.322
F3				
R/G, 2%	0.300	0.037	0.113	0.082
R/G, 3%	0.233	0.041	0.260	0.083
B/G	0.448*	0.049	0.320	0.074
Diagonals	0.237	0.089	0.658*	0.079
CIE isoluminant circle	0.251	0.045	0.192	0.048
Personalized isoluminant circle	0.397*	0.065	0.283	0.055
Cylinder	0.548*	0.035	1.154*	0.136
Overall MSE	0.345	0.052	0.426	0.080
95% confidence limit	0.342	0.299	0.339	0.350

^aResidual errors in the model fits for the fundamental (F1) response and the second-harmonic (F2) response, as mean-squared error (MSE). MSEs are in μV^2 , and confidence limits on the measured responses are determined by the T_{circ}^2 statistic (Victor & Mast, 1991). * denotes sessions for which the residual error in the model fit exceeded the 95% confidence limit.

that the sensitivities (s_R, s_G, s_B) corresponded to a pure luminance mechanism, then the derived triplet of cone contributions (q_L, q_M, q_S) would be proportional (1,1,0). This corresponds to the notion that the S cone does not contribute to luminance, and that the normalizations of Table 3 are such that the photopic luminance V_λ is proportional to the sum of the L- and M-cone responses. This calculation routinely resulted in nonzero values for the S-cone contribution q_S . Since the relative normalizations of the S cone and the two long-wavelength cones in Table 3 are arbitrary, we needed a convention to compare q_S with the contributions q_L and q_M of the L and M cones. We chose to normalize the cone contributions by equating their responses to the "white" background light used in these studies. In these normalized units, the cone contributions are specified by a triplet (Q_L, Q_M, Q_S), where $Q_c = W_c q_c$, and W_c is the response of cone c to a light composed of equal mixtures of R, G, and B gun emissions. W_c can be obtained by summing the rows of the matrix inverse of T_{cp} . The numerical values of (Q_L, Q_M, Q_S) are independent of the relative cone sensitivities of Table 3, but are dependent on the choice of the white point.

The calculation of the triplet of normalized cone contributions (Q_L, Q_M, Q_S) was performed separately for each subject, for both the CIE coordinates and the subject's personalized DKL coordinate

frame. Additionally, normalized cone contributions (Q_L, Q_M, Q_S) were calculated for an ideal luminance mechanism. As with the un-normalized cone contributions (q_L, q_M, q_S), the S-cone contribution for the luminance mechanism is guaranteed to be zero. However, the ratio Q_L/Q_M need not be 1, because of the difference in L- and M-cone sensitivity to white light.

The results of this analysis are shown in the lower half of Table 5. We first consider the long-wavelength cone ratio Q_L/Q_M . In CIE coordinates, there is a 20-fold variability in this ratio, ranging from 1:0.025 (subject RR) to 1:0.57 (subject MC), and for most subjects, these ratios differ from the ratio of 1:0.55 expected for a luminance mechanism. In personalized coordinates, the between-subject variability in this ratio is reduced to approximately fourfold, from 1:0.26 (subject CM) to 1:0.93 (subject MC). Furthermore, across subjects, the average ratio (1:0.56) is very similar to that expected from a pure luminance mechanism (1:0.50). Thus, there does not seem to be a consistent difference between the L- and M-cone contributions to the model mechanism, and their contributions to luminance.

In the standard view, the S cone does not contribute to luminance. However, in all cases, a nonzero contribution Q_S from the S cone was required to reconstruct the model mechanism's sensi-

tivity. This contribution was always positive (i.e. in-phase with that of the L and M cones). In the normalization we have used, it ranged from 0.013 to 0.062 (CIE coordinates) or 0.020 to 0.091 (personalized coordinates). In one sense, this contribution is a small one—the direction of the mechanism in color space is not very different from one in which Q_S is replaced by 0. However, in another sense, it is a very substantial one: the sensitivity to short wavelengths (e.g. near 440 nm) is augmented severalfold by this contribution from the S cone.

Since the identified chromatic sensitivities (s_R, s_G, s_B) are not very different from a pure luminance mechanism, this cannot be the explanation for the failure to identify a null near isoluminance in the R/G or B/G sweep experiments (Fig. 5). That is, even though the color directions in the sweep sessions encompassed the null directions for luminance and the null direction for the derived mechanism, the response was not reduced to zero.

Other qualitative discrepancies between the model and the data are revealed by a more detailed analysis of the pattern of modelling errors. Fig. 6 shows a comparison of measured amplitude and phase for two subjects, and the best-fit model. Qualitatively, the model does a good job of accounting for the small responses measured near the isoluminant plane, and the overall growth of the

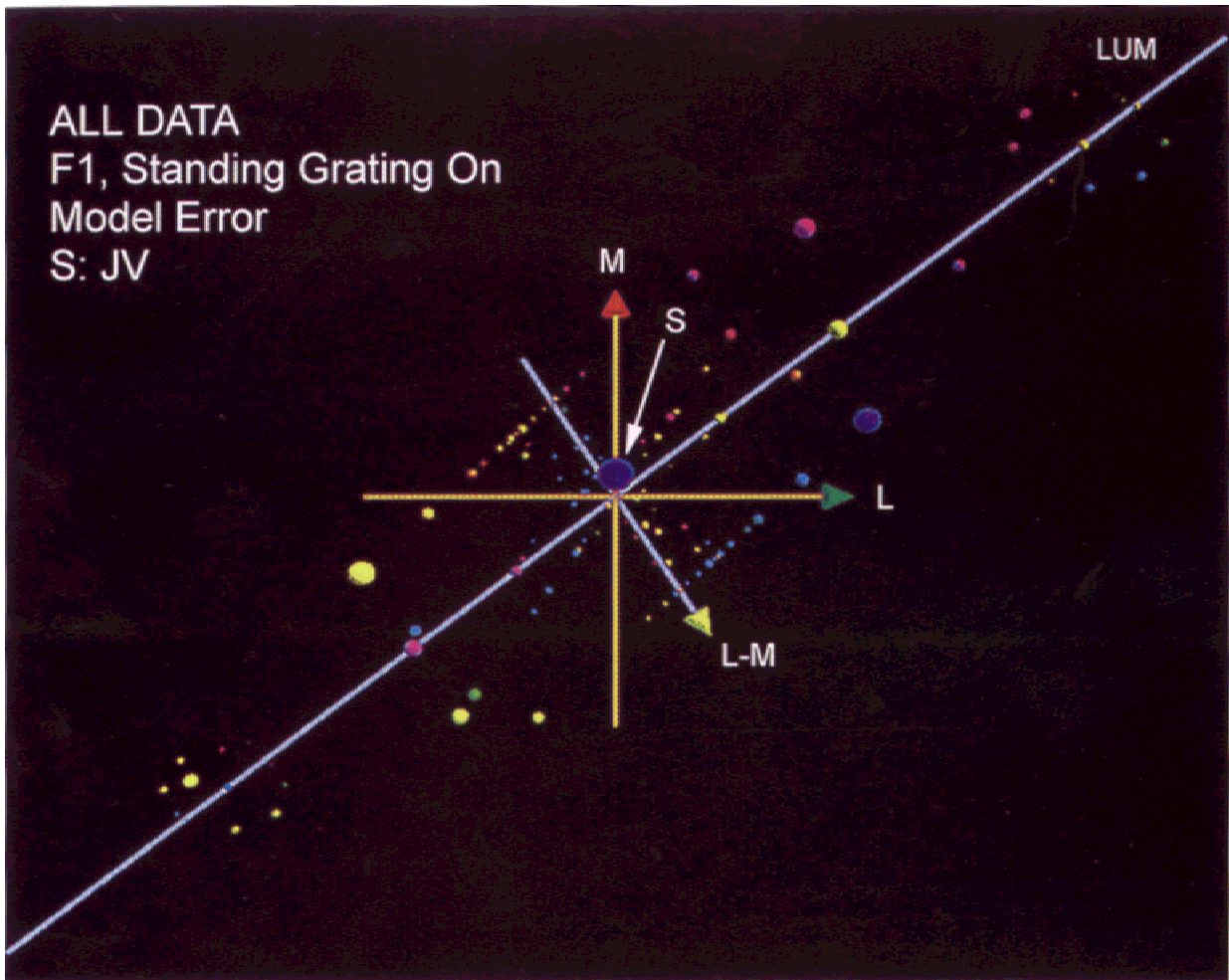


Fig. 7. Comparison of steady-state responses and model fits. The vector difference between the observed and the modelled responses are plotted, with amplitude and phase rendered as in Fig. 6. The space has been transformed so that the personal cone-isolating directions are orthogonal. Subject: JV.

response away from the isoluminant plane. However, there is more variation in the phases of the measured response than can be accounted for by the model, even though the model has the freedom to shift phase as a function of response amplitude. This suggests that the model fails to predict response phase only in certain directions in color space, and not that the functional form chosen for the phase is incorrect.

Additional information concerning the nature of the discrepancy between the model and the experimental data can be obtained from a session-by-session analysis of modelling errors (Table 6). For all subjects except RR (who had the smallest responses), the mean-squared modelling error is larger than the typical response uncertainty, as determined by the T_{circ}^2 statistic. Moreover, the modelling errors are not uniformly distributed, but rather, they are more prominent in certain of the experimental sessions: the R/G sweeps, the B/G sweep, and the diagonals. The model provides a reasonable account of the responses in experiments in which the superimposed chromatic grating was near isoluminance, and in which the superimposed grating contained mixtures of luminance and isoluminant components, but was desaturated (the “cylinder” session).

Fig. 7 shows how the modelling errors are arranged in color space. To focus on the cone mechanisms, we have applied a skew transformation to the color space so that the cone-isolating axes are made orthogonal. This expands the portion of the space devoted to stimuli in which the L and M cones are modulated in antiphase, and moves the points corresponding to the cylinder sessions away from the origin (but keeps them in a tight circle around the luminance axis). Modelling errors are distributed in a systematic way: they are large in the quadrants of space corresponding to in-phase modulation of the L and M cones, and small in the quadrants of space corresponding to antiphase modulation of the long- and middle-wavelength cones. This observation suggests that the original hypothesis of independent processing of color and luminance is wrong in two ways: not only do S cones provide an input to the color-luminance interaction, but also, there appears to be a distinct color-luminance interaction when L and M cones are deeply modulated.

Higher harmonics

The above modelling approach was extended to the higher harmonics of the response. As shown in Figs. 3 and 4, there is a substantial second harmonic (F2) response when the standing chromatic grating is not present—i.e. the contrast-reversal response to the luminance grating. Therefore, as a first approximation to isolation of the color-luminance interactions that contribute to the second harmonic, we considered the vector difference between the second harmonic measured when the chromatic grating was present, and when it was removed. The above model and fitting procedure was used, but with the chromatic sensitivities (s_R, s_G, s_B) held fixed at the values determined by the model for the first harmonic. As seen in Table 6, for the two subjects with the largest second-harmonic responses (CM and MC), the mean-squared error was substantially greater than the uncertainty of the measured responses. However, in contrast to what we observed in the F1 responses, the pattern of errors was more widespread, making a mechanistic interpretation more difficult. Allowing the chromatic sensitivities (s_R, s_G, s_B) to vary did not result in a significant decrease in residuals, or in a consistent shift of the parameter values across subjects. Thus, it appears that one component of the F2 response is indeed generated by a unitary mechanism similar to

that modelled for F1 (but with different amplitude and phase behavior), but that the F2 response also contains additional superimposed processes.

The intersubject variation of the F2 responses also indicates that at least two mechanisms (of different relative strengths across individuals) are involved. For superimposed gratings near isoluminance, subjects MC and CM showed substantial suppression (e.g. 50%) of the F2 response amplitude, but subjects RR and JV showed no significant change. For superimposed gratings which contained large luminance components (e.g. the cylinder sessions), subject MC showed a suppression of the F2 response, while the other three subjects showed an augmentation of the response.

The third harmonic responses were significantly different from zero in three of the subjects (CM, JV, and MC). With chromatic sensitivities (s_R, s_G, s_B) held fixed at the values determined by the model for the first harmonic, residual mean-squared error was within the limits determined by the T_{circ}^2 statistic for subject CM and JV. For subject MC, the distribution of elevated mean-squared errors was widespread, and without an apparent pattern. Only subject MC had a substantial number of fourth harmonic responses that were significantly different from zero. Because of the inability to look for between-subject consistency, F3 and higher harmonics were not examined further.

Discussion

Summary of results

We have examined how the VEP elicited by a contrast-reversing luminance grating is modified by the superposition and withdrawal of standing spatial contrast (with both luminance and chromatic components). The superimposed grating induced a fundamental response component, with time lag of less than 250 ms, and the size of this response was approximately constant throughout the 4-s period in which the superimposed grating was present. The preliminary hypothesis that luminance and chromatic signals are processed independently implied a model for the results, in which the size of the induced fundamental response is determined by the luminance component of the superimposed standing grating, and in which the fundamental response is nulled when the superimposed standing grating is isoluminant. We could approximately account for the size of the induced fundamental response by an interaction between the luminance grating and a mechanism sensitive to the standing grating, but the chromatic sensitivity of this mechanism deviated from that of pure luminance in that there was substantial S-cone input. Despite the overall success of the model in accounting for the pattern of responses, several observations suggested that additional mechanisms were also active. The fundamental response was never nulled, even for standing gratings which occupied a closely spaced trajectory that crossed the null plane of this putative mechanism. Away from the isoluminant plane, the one-mechanism model also failed to account for responses to in-phase L- and M-cone modulations, and generated a smaller repertoire of response phases than was observed experimentally. The one-mechanism model also could not provide a complete account of the higher harmonic responses.

Analysis of cone inputs to the modelled mechanism

Our approach to the analysis of cone inputs to the modelled mechanism was designed to limit possible pitfalls and artifacts. As in previous studies, stimuli were constructed with 2-cycle/deg grat-

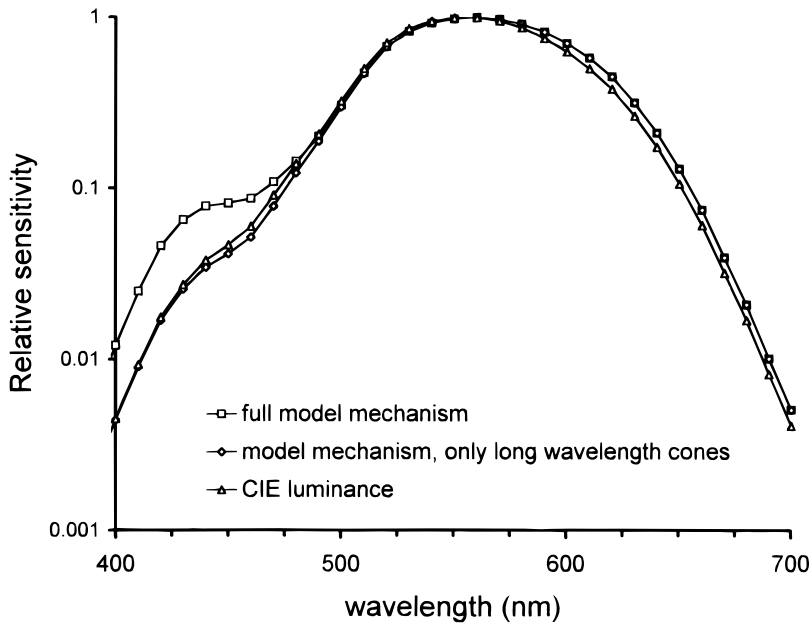


Fig. 8. Derived spectral sensitivities of the modelled mechanism with and without the S-cone contribution and the CIE photopic luminance sensitivity curve. All curves have been normalized to have a peak value of 1.

ings, to limit the effects of chromatic aberration (Rabin et al., 1994).

Our other strategy was to customize the cone fundamentals. Rather than assume that our subjects conformed to CIE standards, or that CIE standards for a central 2-deg spot were appropriate for a large-field grating, we determined empirical luminance matches for the grating stimulus for each of the subjects. These pairwise matches were used to adjust the amount (i.e. effective thickness) of macular and lens absorption, to provide “personalized” cone fundamentals, which exactly accounted for the subjects’ flicker photometric matches. For each subject, we carried out modelling and the analysis of cone contributions both with standard CIE coordinates, and with coordinates derived from these personalized fundamentals.

Across subjects, the relative contribution of the L and M cones has an average which is nearly identical to their contributions to luminance. However, there is much between-subject variability in this ratio (Table 5). This variability is reduced but not eliminated when contributions are calculated from the personalized fundamentals, rather than the CIE standards. Some of this residual variation may be due to assumptions that we have made in the colorimetric calculations, in that we modelled all variability across subjects as changes in preretinal absorption. But other factors may play a role, especially individual differences in photopigment absorption spectra and density (Webster & MacLeod, 1988). There is substantial intersubject variability in the ratio of L and M photoreceptors in the fovea (Cicerone & Nerger, 1989) and parafovea (Nerger & Cicerone, 1992), which are likely to contribute to intersubject differences in flicker photometry (Cicerone, 1990). Additional factors including photopigment gene number (Neitz & Neitz, 1995) and relative synaptic efficacy of the cones may also contribute to receptor-related individual differences in color vision. Finally, the large number of cycles in the display might lead to modest chromatic aberrations in the retinal periphery (Kulikowski et al., 1996), which could be another source of intersubject differences. Thus, we are unable to determine whether this between-subject variability reflects variations in the cone fundamentals, or rather, postreceptor differences in processing.

A distinctive feature of the modelled mechanism is that there is a significant S-cone contribution, which is in phase with (i.e. acts to reinforce) signals from the L and M cones (Table 5), whether the analysis is done in terms of standard or personalized coordinates. The average values for the S-cone contributions listed in Table 5 correspond to a 2.27-fold augmentation in the relative sensitivity to 440 nm (Fig. 8). Above approximately 470 nm, the spectral sensitivity of the derived mechanism is virtually indistinguishable from that of a pure luminance mechanism, whether or not the S-cone contribution is included. The addition of an in-phase S-cone signal to a luminance signal derived from the L and M cones means that (for a given total energy) the optimal spectral distribution for stimulation of the mechanism is shifted from a yellow-appearing light towards white.

The conclusion that there is an S-cone contribution to the interaction of chromatic and luminance gratings is independent of the longstanding controversy of whether the S cone contributes to luminance (Boynton, 1996): if indeed there is an S-cone contribution to luminance, then (since our finding holds even when the analysis is based on empirical flicker photometric matches), a greater S-cone contribution is needed to account for the approximate null plane of the color-luminance interaction. The excess S-cone input can be seen directly from the vector plots of Fig. 5: for both subjects, the point along the trajectory of the B/G sweep which is the closest to the origin corresponds to a greater amount of counterphase G than the point of subjective isoluminance.

Relationship to other noninvasive electrophysiological studies

A number of investigators have used the noninvasive electrophysiological techniques to investigate chromatic processing in man, beginning with Regan (1973), as reviewed in Rabin et al., (1994). These studies have focussed on comparing the timecourse and, to a lesser extent, the scalp distribution of responses elicited by chromatic contrast to responses elicited by luminance contrast. VEP responses elicited by purely chromatic modulation have a distinctive timecourse compared with VEP responses elicited by lumi-

nance modulation: they generally have a longer latency and/or a more prolonged transient component (Murray et al., 1987; Crognale et al., 1993; Rabin et al., 1994). Despite disagreement about the technical requirements for the isolation of a chromatic VEP (Kulikowski et al., 1996; Switkes et al., 1996), there is agreement that chromatic VEPs are more robust at the lower temporal frequencies. The temporally distinctive chromatic VEP responses (for pattern appearance) were prominent for spatial frequencies in the 1–2 cycles/deg range, similar to what was used in these studies to provide standing chromatic contrast. Similar conclusions were reached from an MEG study (Regan & He, 1996), which also emphasized the extent of individual differences that are apparent when details of waveforms are compared.

All of the above studies are based on a conceptual framework in which a stimulus is considered to have chromatic and luminance components, and in which the responses to these components vary independently. In contrast, the present experiments are focussed on the interaction of these components. Our stimulus is a superposition of a temporally modulated luminance grating, and a standing grating which may occupy any of an extensive set of directions in color space. Since our analysis examines the temporally modulated component of the response, we are essentially examining how the luminance signal is modified by the presence of standing chromatic (and luminance) contrast. Since we find clear evidence of interactions, we must conclude that analyses of early visual processing which consider the chromatic and luminance components of the stimulus independently are necessarily incomplete. This is not to deny the value of techniques that isolate individual mechanisms or subsystems (Regan, 1970, 1973; Johnsen et al., 1995), but rather to emphasize that under physiological circumstances, these subsystems cannot be regarded in isolation (Paulus et al., 1986).

Relationship to other studies of interactions of chromatic and luminance signals

A variety of psychophysical studies have provided evidence for interactions of chromatic and luminance signals in low-level visual tasks. For example, a luminance pedestal facilitates the detection of a chromatic flash, and a chromatic pedestal facilitates the detection of a luminance flash (Cole et al., 1990). In studies of spatial contrast produced by gratings (Switkes et al., 1988) and edges (Eskew et al., 1991, 1994), the presence of a luminance contour enhances detection of a chromatic difference, but there is minimal effect of a chromatic grating on detection of a luminance grating (Switkes et al., 1988). This facilitatory effect of luminance contours on the detection of chromatic contours is in contrast to the threshold elevation produced when target and mask signals are either both luminance or both chromatic (Bradley et al., 1988). Indeed, one possibility is that there is a global masking both within and across categories, which is mitigated or even reversed by facilitatory interactions between chromatic and luminance signals. This view would also account for the studies of lateral interactions of dynamic contrast (Singer et al., 1993; D'Zmura et al., 1995; Singer & D'Zmura, 1994, 1995), in which an annular patch of contrast (either luminance or chromatic) reduced the contrast of a central region, but this reduction was greatest when the surrounding patch and the central patch were either both luminance or both chromatic.

Mullen (1987) identified a contribution of a color-opponent mechanism to detection of monochromatic gratings at low spatial frequencies, when superimposed on a sufficiently bright white back-

ground. This interaction was eliminated by dichoptic stimulation, suggesting a precortical origin. However, although the Mullen study and the present one both concern an interaction of achromatic and chromatic signals, the former study examined interaction of color-opponent signals with luminance changes, while our study focuses on contrast modulation in the absence of luminance changes.

Stockman et al. (1993) demonstrated an S-cone contribution to luminance, *via* detection of a beat generated by an interaction of rapidly modulated (10 to 40 Hz) S-cone signals and signals generated by long-wavelength cones. The extrapolated phase of this S-cone signal to 0 frequency would result in a contribution to luminance which is antagonistic to the long-wavelength luminance signal—not the reinforcing contribution that we found here. Most likely, the two techniques reveal distinct interactions: our method would not be sensitive to signals at high temporal frequencies, and the Stockman et al. (1993) approach could not be applied at low temporal frequencies.

The interaction of chromatic and luminance signals we observed is clearly distinct from a luminance gain control, even with some “leakage” of chromatic signals into a luminance channel. The average luminance contrast shifts the contrast-response function of the contrast-reversal VEP (Victor et al., 1997). This shift due to luminance contrast reflects the amount of contrast over a relatively long period of time (*ca.* 700 ms). A similar adaptive shift with corresponding dynamics has recently been observed in the human pattern ERG (Conte et al., 1997), indicating that it has a retinal locus. However, the dynamics of the processes observed here (induction of the fundamental within the measurement window of 237 ms and no subsequent decline) indicate that the chromatic/luminance interaction is a distinct one.

Possible neurophysiological basis of our findings

Given the multitude and complexity of generators underlying the visual evoked potential, one cannot deduce the cellular origins of the interactions we have observed from the features of the responses. Nevertheless, previous studies of retinal ganglion cells and LGN neurons permit us to hypothesize some likely possibilities. Our model indicates that mixtures of static chromatic and luminance contrast interact with a contrast-reversing grating much as had been observed by Bodis-Wollner et al. (Bodis-Wollner et al., 1972; Bobak et al., 1988), for luminance gratings, except that the measure of static contrast is not along a pure luminance axis, but rather, along an axis that has additional S-cone weighting. This implies that prior to the site of generation of the VEP, the “luminance” signal, operationally defined as that which nulls during heterochromatic flicker photometry, has been modified by the addition of S-cone signals. These S-cone signals might be transmitted by the parvocellular pathway, or by the newly identified K, or intralaminar, pathway (Hendry & Yoshioka, 1994; Martin et al., 1997; Reid et al., 1997). Recent evidence suggests that cortical combination of S signals with geniculate-derived L and M signals is the rule, rather than the exception (DeValois et al., 1997). However, it is unclear if this new luminance-like signal replaces the traditional luminance signal at later processing stages, or coexists with it.

In addition to this axis shift, we found indications of other kinds of interactions, particularly when L- and M-cone signals are modulated in phase. Most studies of chromatic properties of neurons at the level of the lateral geniculate and retina have utilized stimuli which were modulated in only a single direction in color space, and thus do not directly address the issue of interaction among

cone classes (Derrington et al., 1984; Lee et al., 1989; Reid & Shapley, 1992). However, quantitative studies of whether cone signals combine additively reveal significant departures from linearity, especially in P cells (Benardete, 1994). Of note, this departure is most marked in situations when L- and M-cone signals are in phase, which coincides with the most prominent departure from our model (Fig. 7). Furthermore, the interaction of light adaptation and chromatic processing (Yeh et al., 1996) necessarily implies that cone signals interact in a nonadditive fashion at the retinal level.

Further interactions between cone signals, and between chromatic and luminance pathways, may occur at the cortical level. This is suggested by interocular transfer of induced chromatic contrast effects (Singer & D'Zmura, 1994). Unfortunately, neurophysiologic studies of chromatic inputs to cortical receptive fields (Lennie et al., 1990; Cottaris et al., 1996) also were restricted to stimuli which were modulated in only a single direction in color space, and thus would not reveal such interactions.

Relationship to gain controls

The emergence of a fundamental response when static spatial contrast (luminance and/or chromatic) is added to a reversing grating is not readily explained by a "gain control" mechanism at the cortical level (Albrecht & Hamilton, 1982; Ohzawa et al., 1982; Albrecht et al., 1984; Ohzawa et al., 1985; Sclar et al., 1989). As identified in these physiologic studies, the cortical contrast gain control assays contrast over time periods measured in seconds and reduce response size when this measured contrast level is high. Such a reduction in gain might contribute to a reduced size of the F2 response seen in some subjects, especially if the cortical contrast gain control is also activated by isoluminant patterns. However, no matter what its chromatic sensitivity, these gain controls would not be expected to lead to a fundamental response to superimposed pattern reversal, since the effective gain (as set by a sluggish measure of contrast) would be identical for both phases of the reversal.

The faster retinal gain control (Shapley & Victor, 1981) is a likely contributor to the emergence of the fundamental response. When the superimposed grating is present, the modulated grating alternates between phases of high and low effective contrast, depending on whether it is in phase or out of phase with the luminance component of the superimposed grating. Alternation between these two states will lead to different gains at the retinal level, whose gain control adjusts within 100 ms (Victor, 1987). Thus, responses to the two reversal phases will be asymmetric, and a net fundamental response will result. However, a simple achromatic retinal gain control cannot account for the S-cone contribution to the "luminance" signal, nor for the interactions between the long wavelength cones.

Functional implications

Despite the uncertainty as to their precise cellular origins, our two main findings have clear functional implications. The identification of a modification of a luminance signal by S-cone inputs is clear evidence for an interaction between "chromatic" pathways and "luminance" pathways. The central luminance signal must be more complex than an L + M cone signal carried by the magnocellular pathway: it is either modified by an S-cone input, or coexists and interacts with a second luminance signal with S-cone input.

The general facilitatory nature of the influence of chromatic contrast on luminance processing may have an important role in the parsing of visual images. The visual system must distinguish between edges generated by object boundaries, and luminance changes generated by shadow edges and/or curvature in depth. Object boundaries generally are associated with color differences, but luminance changes generated by shadows and curvature typically are not. Thus, a facilitatory influence of chromatic contrast on the detection of luminance contrast may be part of a larger computational strategy to extract the boundaries of objects.

Acknowledgments

We thank Rahil Rahim for her technical assistance, and we thank Jim Gordon and Israel Abramov for their assistance with color measurements. A portion of this work was presented at the 1996 meeting of the Association for Research in Vision and Ophthalmology in Ft. Lauderdale, FL (Victor et al., 1996). This work was supported by NIH Grant EY7977 (J.D.V.) and NS01677 (K.P.P.).

References

- ALBRECHT, D.G. & HAMILTON, D.B. (1982). Striate cortex of monkey and cat: Contrast response function. *Journal of Neurophysiology* **48**, 217–237.
- ALBRECHT, D.G., FARRAR, S.B., & HAMILTON, D.B. (1984). Spatial contrast adaptation characteristics of neurons recorded in the cat's visual cortex. *Journal of Physiology* **347**, 713–739.
- BENARDETE, E.A. (1994). *Functional dynamics of primate retinal ganglion cells*. Thesis, The Rockefeller University, New York.
- BENARDETE, E.A., KAPLAN, E. & KNIGHT, B.W. (1992). Contrast gain control in the primate retina: P cells are not X-like, some M cells are. *Visual Neuroscience* **8**, 483–486.
- BLACKWELL, K.T. & BUCHSBAUM, G. (1988). Quantitative studies of color constancy. *Journal of the Optical Society of America* **A5**, 1772–1780.
- BOBAK, P., BODIS-WOLLNER, I. & MARX, M.S. (1988). Cortical contrast gain control in human spatial vision. *Journal of Physiology* **405**, 421–437.
- BODIS-WOLLNER, I., HENDLEY, C.D. & KULIKOWSKI, J.J. (1972). Psychophysical and electrophysiological responses to the modulation of contrast of a grating pattern. *Perception* **1**, 341–349.
- BOYNTON, R.M. (1979). *Human Color Vision*. New York: Holt, Rinehart, and Winston.
- BOYNTON, R.M. (1996). History and current status of a physiologically based system of photometry and colorimetry. *Journal of the Optical Society of America* **A13**, 1609–1621.
- BRADLEY, A., SWITKES, E. & DEVALOIS, K. (1988). Orientation and spatial frequency selectivity of adaptation to color and luminance gratings. *Vision Research* **28**, 841–856.
- BRAINARD, D.H. & WANDELL, B.A. (1992). Asymmetric color matching: How color appearance depends on the illuminant. *Journal of the Optical Society of America* **A9**, 1433–1448.
- CICERONE, C.M. (1990). Color appearance and the cone mosaic in trichromacy and dichromacy. In *Color Vision Deficiencies*, ed. OHTA, Y., pp. 1–12. Amsterdam: Kugler & Ghedini.
- CICERONE, C.M. & NERGER, J.L. (1989). The relative numbers of long-wavelength-sensitive to middle-wavelength-sensitive cones in the human fovea centralis. *Vision Research* **29**, 115–128.
- COLE, G.R., STROMEYER III, C.F. & KRONAUER, R.E. (1990). Visual interactions with luminance and chromatic stimuli. *Journal of the Optical Society of America* **A7**, 128–140.
- CONTE, M.M., BRODIE, S.E. & VICTOR, J.D. (1997). Retinal contribution to contrast adaptation in human vision. *Investigative Ophthalmology and Visual Science* (Suppl.) **38**, 627.
- COTTARIS, N.P., EL FAR, S.D. & DEVALOIS, R.L. (1996). Spatiotemporal luminance and chromatic receptive field profiles of macaque striate cortex simple cells. *Society for Neuroscience Abstracts* **22**, 951.
- CROGNALÉ, M.A., SWITKES, E., RABIN, J., SCHNECK, M.E., HEGERSTRÖM-PORTNOY, G. & ADAMS, A.J. (1993). Application of the spatiochromatic visual evoked potential to detection of congenital and acquired color-vision deficiencies. *Journal of the Optical Society of America* **A10**, 1818–1825.

- DERRINGTON, A.M., KRAUSKOPF, J. & LENNIE, P. (1984). Chromatic mechanisms in lateral geniculate nucleus of macaque. *Journal of Physiology* **357**, 241–265.
- DEVALOIS, R.L., COTTARIS, N.P. & EL FAR, S.D. (1997). S-cone inputs to striate cortex cells. *Investigative Ophthalmology and Visual Science* (Suppl.) **38**, 15.
- D'ZMURA, M., SINGER, B. & LI, C.-H. (1995). A bilinear model for contrast gain control. *Investigative Ophthalmology and Visual Science* (Suppl.) **36**, 392.
- ESKEW, R.T., STROMEYER, III, C.F. & KRONAUER, R.E. (1994). The time-course of chromatic facilitation by luminance contours. *Vision Research* **34**, 3139–3144.
- ESKEW, R.T., STROMEYER, III, C.F., PICOTTE, C.J. & KRONAUER, R.E. (1991). Detection uncertainty and the facilitation of chromatic detection by luminance contours. *Journal of the Optical Society of America* **A8**, 394–403.
- HENDRY, S.H.C. & YOSHIOKA, T. (1994). A neurochemically distinct third channel in the macaque dorsal lateral geniculate nucleus. *Science* **264**, 575–577.
- JOHNSON, B., FREDERIKSEN, J.L. & LARSSON, H.B.W. (1995). Comparison of the pattern reversal visual evoked potential mediated by separate cone systems. *Electroencephalography and Clinical Neurophysiology* **96**, 97–104.
- KULIKOWSKI, J.J., ROBSON, A.G. & MCKEEFRY, D.J. (1996). Specificity and selectivity of chromatic visual evoked potentials. *Vision Research* **36**, 3397–3401.
- LEE, B.B., MARTIN, P.R. & VALBERG, A. (1989). Sensitivity of macaque retinal ganglion cells to chromatic and luminance flicker. *Journal of Physiology* **414**, 223–243.
- LENNIE, P., KRAUSKOPF, J. & SCLAR, G. (1990). Chromatic mechanisms in striate cortex of macaque. *Journal of Neuroscience* **10**, 649–669.
- MARTIN, P.R., WHITE, A.J.R., GOODCHILD, A.K. & WILDER, H. (1997). Blue-on cells are part of the third geniculocortical pathway in a new world monkey, the marmoset *Callithrix jacchus*. *Investigative Ophthalmology and Visual Science* (Suppl.) **38**, 363.
- MILKMAN, N., SCHICK, G., ROSSETTO, M., RATLIFF, F., SHAPLEY, R. & VICTOR, J.D. (1980). A two-dimensional computer-controlled visual stimulator. *Behavioral Research Methods and Instrumentation* **12**, 283–292.
- MULLEN, K.T. (1987). Spatial influences of colour opponent contributions to pattern detection. *Vision Research* **27**, 829–839.
- MURRAY, I.J., PARRY, N.R.A., CARDEN, D. & KULIKOWSKI, J.J. (1987). Human visual evoked potentials to chromatic and achromatic gratings. *Clinical Vision Sciences* **1**, 231–244.
- NAIMAN, A.C. & MAKOUS, W. (1992). Spatial non-linearities of grayscale CRT pixels. *SPIE Human Vision, Visual Processing, and Digital Display* **1666**, 41–46.
- NEITZ, M. & NEITZ, J. (1995). Numbers and ratios of visual pigment genes for normal red-green color vision. *Science* **267**, 1013–1016.
- NERGER, J.L. & CICERONE, C.M. (1992). The ratio of L cones to M cones in the human parafoveal retina. *Vision Research* **32**, 879–888.
- OHZAWA, I., SCLAR, G. & FREEMAN, R.D. (1982). Contrast gain control in the cat visual cortex. *Nature* **298**, 266–268.
- OHZAWA, I., SCLAR, G. & FREEMAN, R.D. (1985). Contrast gain control in the cat's visual system. *Journal of Neurophysiology* **54**, 651–667.
- PAULUS, W.M., HÖMBURG, V., CUNNINGHAM, K. & HALLIDAY, A.M. (1986). Colour and brightness coding in the central nervous system: Theoretical aspects and visual evoked potentials to homogeneous red and green stimuli. *Proceedings of the Royal Society B (London)* **227**, 53–66.
- PELLI, D. & ZHANG, L. (1991). Accurate control of contrast on microcomputer displays. *Vision Research* **31**, 1337–1350.
- PURPURA, K. & VICTOR, J.D. (1990). Dissociation of cortical form mechanisms and spatial filtering at isoluminance. *Investigative Ophthalmology and Visual Science* (Suppl.) **31**, 265.
- RABIN, J., SWITKES, E., CROGNALE, M., SCHNECK, M.E. & ADAMS, A.J. (1994). Visual evoked potentials in three-dimensional color space: Correlates of spatio-chromatic processing. *Vision Research* **34**, 2657–2671.
- REGAN, D. (1970). Objective method of measuring the relative spectral-luminosity curve in man. *Journal of the Optical Society of America* **60**, 856–859.
- REGAN, D. (1973). Evoked potentials specific to spatial patterns of luminance and colour. *Vision Research* **13**, 1933–1941.
- REGAN, D. (1989). *Human Brain Electrophysiology*. New York: Elsevier.
- REGAN, D. & HE, P. (1996). Magnetic and electrical brain responses to chromatic contrast in human. *Vision Research* **36**, 1–18.
- REID, R.C., ALONSO, J.-M. & HENDRY, S.H.C. (1997). S-cone input is relayed to visual cortex from two konio-cellular layers of macaque LGN. *Society for Neuroscience Abstracts* **23**, 13.
- REID, R.C. & SHAPLEY, R.M. (1992). Spatial structure of cone inputs to receptive fields in primate lateral geniculate nucleus. *Nature* **356**, 716–718.
- REID, R.C., VICTOR, J.D. & SHAPLEY, R.M. (1992). Broad-band temporal stimuli decrease the integration time of neurons in cat striate cortex. *Visual Neuroscience* **9**, 39–45.
- SCHNAPF, J.C., KRAFT, T.W. & BAYLOR, D.A. (1987). Spectral sensitivity of human cone photoreceptors. *Nature* **325**, 439–441.
- SCLAR, G., LENNIE, P. & DEPRIEST, D.D. (1989). Contrast adaptation in striate cortex of macaque. *Vision Research* **29**, 747–755.
- SHAPLEY, R.M. & ENROTH-CUGELL, C. (1984). Visual adaptation and retinal gain controls. *Progress in Retinal Research* **3**, 263–346.
- SHAPLEY, R. & VICTOR, J.D. (1978). The effect of contrast on the transfer properties of cat retinal ganglion cells. *Journal of Physiology* **285**, 275–298.
- SHAPLEY, R. & VICTOR, J.D. (1979). The contrast gain control of the cat retina. *Vision Research* **19**, 431–434.
- SHAPLEY, R. & VICTOR, J.D. (1981). How the contrast gain control modifies the frequency response of cat retinal ganglion cells. *Journal of Physiology* **318**, 161–179.
- SINGER, B., HAN, K.-H. & D'ZMURA, M. (1993). Color selectivity in contrast gain control. *Investigative Ophthalmology and Visual Science* (Suppl.) **34**, 764.
- SINGER, B. & D'ZMURA, M. (1994). Color contrast induction. *Vision Research* **34**, 3111–3126.
- SINGER, B. & D'ZMURA, M. (1995). Contrast gain control. A bilinear model for chromatic selectivity. *Journal of the Optical Society of America* **A12**, 667–685.
- SMIRNAKIS, S.M., BERRY, M.J., WARLAND, D.K., BIALEK, W. & MEISTER, M. (1997). Adaptation of retinal processing to image contrast and spatial scale. *Nature* **386**, 69–73.
- SMITH, V.C. & POKORNY, J. (1975). Spectral sensitivity of the foveal cone photopigments between 400 and 500 nm. *Vision Research* **15**, 161–171.
- SPEKREIJSE, H., VAN DER TWEEL, L.H. & ZUIDEMA, T. (1973). Contrast evoked responses in man. *Vision Research* **13**, 1577–1601.
- STOCKMAN, A., MACLEOD, D.I.A. & LEBRUN, S.J. (1993). Faster than the eye can see: Blue cones respond to rapid flicker. *Journal of the Optical Society of America* **A10**, 1396–1402.
- SWITKES, E., BRADLEY, A. & DEVALOIS, K.K. (1988). Contrast dependence and mechanisms of masking interactions among chromatic and luminance gratings. *Journal of the Optical Society of America* **A5**, 1149–1162.
- SWITKES, E., CROGNALE, M., RABIN, J., SCHNECK, M.E. & ADAMS, A.J. (1996). Reply to "Specificity and selectivity of chromatic visual evoked potentials." *Vision Research* **36**, 3403–3405.
- VICTOR, J.D. (1987). The dynamics of the cat retinal X cell centre. *Journal of Physiology* **386**, 219–246.
- VICTOR, J.D., CONTE, M.M. & PURPURA, K.P. (1997). Dynamic shifts of the contrast-response function. *Visual Neuroscience* **14**, 577–587.
- VICTOR, J.D., CONTE, M.M., RAHIM, R. & PURPURA, K.P. (1996). Facilitatory interactions of chromatic and luminance signals in man. *Investigative Ophthalmology and Visual Science* (Suppl.) **37**, 3.
- VICTOR, J.D. & MAST, J. (1991). A new statistic for steady-state evoked potentials. *Electroencephalography and Clinical Neurophysiology* **78**, 378–388.
- WALRAVEN, J., ENROTH-CUGELL, C., HOOD, D., MACLEOD, D.I.A. & SCHNAPF, J. (1990). The control of visual sensitivity: Receptor and postreceptor processes. In *Visual Perception: The Neurophysiological Foundations*, ed. SPILLMAN, L. & WERNER, J., pp. 53–101. New York: Academic Press.
- WANDELL, B.A. (1995). *Foundations of Vision*. Sunderland, Massachusetts: Sinauer Associates.
- WEBSTER, M.A. & MACLEOD, D.I.A. (1988). Factors underlying individual differences in the color matches of normal observers. *Journal of the Optical Society of America* **A15**, 1722–1735.
- WEBSTER, M.A. & MOLLON, J.D. (1995). Color constancy influenced by contrast adaptation. *Nature* **373**, 694–698.
- WYSZECKI, G. & STILES, W.S. (1967). *Color Science: Concepts and Methods, Quantitative Data and Formulas*. New York: Wiley.
- YEH, T., LEE, B.B. & KREMERS, J. (1996). The time course of adaptation in macaque retinal ganglion cells. *Vision Research* **36**, 913–931.